Spring 2024

PLANT WATER UPTAKE STRATEGIES IN AN URBAN GREEN LANDSCAPE

Erica G. Almance
University of Texas at Arlington

PLANT WATER UPTAKE STRATEGIES IN AN URBAN GREEN LANDSCAPE

by

ERICA G. ALMANCE

THESIS

Submitted in Partial Fulfillment

of the Requirements

for the Degree of

MASTER OF SCIENCE IN EARTH AND ENVIRONMENTAL SCIENCES

THE UNIVERSITY OF TEXAS AT ARLINGTON

May 2024

Acknowledgments

I would like to thank the Fort Worth Botanic Garden and the Botanical Research Institute of Texas for providing access to an experimental plot within the south woods of the botanic gardens, assistance with plant identification, and enthusiastic support of our project. The authors also recognize the support from the UT System STARs Program (No. AR911486) and the Office of the Provost funds at the University of Texas-Arlington (No. 314075).

Dedication

I'd like to dedicate this to my father, Jose Almance, who supported me before I even existed. To my mother, Edith Almance, who shows me her support every day through her existence everlasting. To my best friend Karissa Cordero, who taught me the true meaning of the bond. To my colleagues and friends in the Tracer Hydrology Group: Alexandra, Charity, Christine, Emma, Juan, Katy, Sahithi, Suprina, and our professor and friend, Ricardo; thank you for your endless encouragement and hard work. To my dear friends Paul and Lori, who have always nurtured and inspired my reverence for nature. To my beloved aunts, Gracie, Jessie, and Tencha; you are my examples of strong women. Finally, to my boyfriend, Joey Benavides. You've been my source of strength; thank you for always believing in me.

Abstract

PLANT WATER UPTAKE STRATEGIES IN AN URBAN GREEN LANDSCAPE

Erica G. Almance, MS

The University of Texas at Arlington, 2024

Supervising Committee:

Ricardo Sanchez-Murillo, Supervising Professor

Brooke Best

Maije Fan

Cornelia Winguth

Urban green landscapes have been widely recognized for potentially reducing surface water pollution and flood impacts. However, the understanding of the role that plants play in partitioning the urban water cycle is still limited. We present a study in the Fort Worth Botanic Garden to understand water uptake strategies from three common urban tree species (Elderberry, *Sambucus canadensis*; Cherry laurel, *Prunus caroliniana*; and Boxelder maple, *Acer negundo*) from February 2023 through January 2024. Stem (N=110) isotope ratios ($\delta^{18}O$ and $\delta^{2}H$) are compared to multiple endmembers, including precipitation (N=509), throughfall (N=37), and soil water (N=135) at different depths (0-38 cm). Water from discrete xylem and soil samples was extracted via high-speed

centrifugation. In addition, soil water samples were obtained from suction lysimeters (N=45) (0-38 cm). Soil and plant water extraction volumes ranged from ~100 µL to 7.5 mL in stem samples and from ~100 µL to 10.5 mL in soil samples. Stem mean narrowband and broadband (proxy for organic contamination) were 0.23±0.40 [-] and 1.00±0.01 [-], respectively. These values agree with mean narrowband and broadband metrics from throughfall and soils. Mean soil $\delta^{18}O$ compositions (-3.55±1.72‰) correspond with the throughfall input (-3.60±2.40‰). Stem $\delta^{18}O$ compositions exhibited a strong temporal trend from high isotope variability at the end of the winter and summer seasons with more uniform isotope ratios during the growing season (spring). Bayesian mixing analysis showed source water contributions were shallow soil (0cm and 12.7cm) for Boxelder Maple, shallow to deep soil (12.7cm and 25.4cm) for Cherry Laurel, and, remarkably, deep soil (25.4cm and 38.1cm) for Elderberry. Our results contribute to the understanding of water extraction analytical procedures and plant water uptake strategies in a highly altered urban landscape.

Table of Contents

Table of Figures

Chapter 1: Introduction

For decades, cryogenic extraction has been used as the reference method to obtain soil and plant water for δ^2H and $\delta^{18}O$ analysis in eco-hydrological studies (e.g., Jusserand, 1980; Dalton et al., 1989; Brooks et al., 2010; Koeniger et al., 2011; Orlowski et al., 2013). From a physicochemical perspective, cryogenic vacuum distillation is an invasive water extraction technique that certainly results in high water extraction efficiencies (Wen et al., 2022). However, in soil and plant samples, the cryo-extracted water inexorably reflects a combination (of unknown proportions) between chemically bounded water (i.e., immobile mineralogical or biological water), soil/xylem mobile water (i.e., the analyte of interest involved in the evapotranspiration process) (Gaj et al., 2017; von Freyberg et al., 2020), and potentially enhance isotope exchange between xylem water and non-crystalline hydroxyl groups of wood cellulose and hemicellulose (Younger et al., 2024).

Cryogenic extraction, despite its wide application, presents a significant challenge in the form of a large spectrum of secondary organic substances (e.g., VOCs, alcohols, and hydrocarbons such as sugars) in the water analyte. These substances are often difficult to separate or eliminate by filtration or properly corrected by standard post-software laser spectroscopy procedures (Wassenaar et al., 2018). As evidence of these challenges, a growing body of scientific literature points towards substantial analytical biases in cryogenic-based extraction when determining soil and xylem isotopic compositions (e.g., Orlowski et al., 2016; Chen et al., 2020; Allen and Kirchner, 2022; Song et al., 2021; Wen et al., 2022; Zuecco et al., 2022; Yang et al., 2023; Wen et al., 2023; Sobota et al., 2024; Younger et al., 2024; Duvert et al., 2024; Ceperley et al., 2024).

Laboratory experiments have also shown that labeled water used in spike tests could not be reliably recovered due to the inherent wetting and drying processes in the soil matrix (Thielemann et al., 2019), resulting in unexpected enrichments or depletions.

The advent of laser spectroscopy (i.e., lower analytical cost and faster injection and integration times, 2-10 minutes, when compared to Isotope Ratio Mass Spectrometry) has motivated the introduction of new in-house and field extraction techniques, such as vapor equilibration, centrifugation, cavitron, microwave in-line distillation, Scholander pressure chamber, high-pressure mechanical squeezing, passive lysimeters, and hygroscopic salt of a high water absorbance capacity ($CaCl_2$) (Fischer et al., 2019; Millar et al., 2022; Zuecco et al., 2022; He et al., 2023; Duvert et al., 2024; El-Shenawy et al., 2024). While these new extraction techniques offer a large potential in decreasing the analytical bias by intricating fractionation and exchange processes during low-volume invasive cryogenic extractions (few mL to ~1 mL; extraction volumes are rarely provided as part of the analytical metadata), there is still a lack of standard operating protocols to conduct robust inter-comparisons, as clearly pointed out in recent reviews by Millar et al. (2022) and Ceperley et al. (2024).

In this regard, a large conundrum exists to a) underpin the ratio of mobile and immobile soil/xylem water relative to the total water contained in a particular sample and b) how this extraction ratio and analytical-induced fractionation bias may alter (either in a depletion or enrichment direction) the ‘true’ isotopic value of water flowing through soil and xylem at a given time. Currently, all available extraction methods are unable to clearly distinguish the relative proportions of immobile/mobile in the extracted water and how this ratio is affecting the relative sample position in the dual-isotope space, consequently

introducing errors in further calculations and modeling results. Even continuous vapor measurements deal with multiple unresolved aspects (Gralher et al., 2021), such as unknown diffusion processes with chemically bounded water and volatile organic compounds in the analyte matrix, dilution correction procedures, or gas blending with pre-sample vapor (Herbstritt et al., 2023). Nonetheless, polymer science techniques, such as Differential Scanning Calorimetry (DSC), could provide valuable information on the sorption, diffusion, and permeation of water in hydrophilic plant tissues. In this regard, the crystallization and the ice melting temperature of free water and freezable bound water can be measured at 0°C and at lower temperatures, respectively. By considering the melting enthalpy (ΔH) of the type of water (chemical bounded vs. free or mobile water) and the heat absorbed during the melting process, the mass of each water type can be obtained (Ping, et al., 2021).

Currently, constraining the pressure applied to extract the water offers the best physically based parameter to discriminate water extraction types. Clearly, cryogenic extractions combine residual moisture at higher tension or beyond the xylem limits and mobile water versus extracting water in the plant-available region (between field capacity and wilting point) via centrifugation. As the main ecohydrological goal is to separate mobile water effectively, extraction pressures are relevant and should be considered when selecting water extraction methods. Commonly, the applied tension in cryogenic extraction is greater than 100 MPa (Sprenger et al., 2015), while porous cup samplers or lysimeters extract mobile water at tensions lower than 200kPa (Geris et al., 2015). Based on the water density, rotational velocity, and the radius of a commonly used centrifugation system (Sánchez-Murillo et al., 2023), a tension of ~2.4 MPa (i.e., between field capacity

and wilting point) is applied, providing a more reliable water extract analyte targeting mobile water.

Here, we present a study in a subtropical urban landscape in north-central Texas (USA) to a) evaluate the consistency and robustness of the centrifugation procedure (previously tested in the wet tropics of Central America; Sánchez-Murillo et al., 2023) in a water-stressed setting, and b) reveal water uptake strategies from three common urban species (Elderberry, *Sambucus canadensis*; Cherry laurel, *Prunus caroliniana*; and Boxelder maple, *Acer negundo*), during an unprecedented warm period (2023-2024) under the influence of a strong El Niño event. Urban green landscapes have been widely recognized for potentially reducing surface water pollution and flood impacts (Barbedo et al., 2014; Lourenço et al., 2020; Green et al., 2021). However, understanding of the role that plants play in partitioning the urban water cycle is still limited. Monthly stem samples (for one year) are compared with throughfall and soil and passive lysimeter samples (at different depths) under a Bayesian mixing model framework. Our results contribute to the global debate on water extraction analytical procedures for stable isotope analysis (based on laser spectroscopy) and to the understanding of plant water uptake strategies across three representative plant species in a highly altered urban landscape.

Chapter 2: Site Description

The Fort Worth Botanic Garden is a 120-acre (0.48 km^2) temperate deciduous forest in Fort Worth, Texas, within the Cross Timbers ecoregion (Griffith et al., 2004). The Botanic Garden lies within the Trinity River watershed, specifically the Clear Fork tributary. Historically, the site was within the Trinity River floodplain, but channelization and levee projects have altered the river's natural hydrologic patterns and affected riparian vegetation (Best, 2021). The predominant soil types are loam and clay. The site has a humid subtropical climate with hot, humid summers and mild winters. Based on a 30-year normal period, the mean annual (high-low) temperature varies between 24.9°C and 13.6 °C, respectively (U.S. Department of Commerce, 2024). The city experiences high temperatures in the summer, often exceeding 32.2°C and sometimes reaching over 37.8°C (U.S. Department of Commerce, 2023). Average annual precipitation is 940 mm, with wet spring and fall seasons and drier summer and winter seasons. Most annual rainfall in the region comes from frontal storms in spring and fall and convection during summer (TWDB, 2012). Summer thunderstorms are generated by the Gulf of Mexico breeze and subtropical disturbances. During spring and fall, warm, dry air from northern Mexico collides with humid air from the Gulf of Mexico due to the forcing of the jet stream and Bermuda High System. This collision leads to severe thunderstorms and tornadoes. Thunderstorms are common, especially in the spring and summer months. The city occasionally experiences severe weather, including tornadoes, hail, and damaging winds up to about 129 km/h. Most of the annual rainfall in Texas originates from storms like these, with flashy episodes of heavy precipitation inputs. On average, however, evaporation exceeds precipitation. The average annual potential evapotranspiration in

Fort Worth is 118.1 mm (Texas A&M AgriLife Extension, 2024). The El Niño Southern Oscillation (ENSO) has long-term influences on Texas precipitation, with above-average precipitation occurring during El Niño and below-average precipitation and drought occurring during La Niña conditions.

Figure 1: *Experimental site location map. The left panel (A) shows the location of the Dallas-Fort Worth Metroplex within north-central Texas, USA. Aerial images of winter (B) vs. summer (C) show the location of the monitoring plot (red pin) within the south woods of the Fort Worth Botanic Gardens within the floodplain of the Clear Fork Trinity River.*

Chapter 3: Methods and materials

3.1. Precipitation and throughfall collection

Weekly throughfall samples (N=37) were collected from a 3L RS1 Palmex passive collector (Palmex Ltd., Croatia; Gröning et al., 2012) installed beneath the canopy one meter above the ground. Similarly, daily regional precipitation samples (N=509) were collected at the University of Texas at Arlington Earth and Environmental Sciences building in Arlington, Texas. The precipitation volume was measured using a 1,000 mL graduated cylinder and converted to mm using the funnel area. The water was then poured to fill a 30 mL HDPE bottle labeled with the location, time, date, and volume of precipitation. Samples were capped (no headspace), sealed with Parafilm, and transported to the lab in a cooler with ice gel packs at approximately 5°C. Fort Worth weather data was collected from the NOAA Climate Data Online website from station USW00013911 (Latitude/Longitude: 32.76667°, -97.45°; Elevation: 185.3 m) (NCEI 2024).

3.2. Ceramic cup sampler installation and soil water collection

Slim tube ceramic cup samplers (Model 1905L, SoilMoisture Equipment Corporation, United States) were installed at depths of 12.7 cm (5 in), 25.4 cm (10 in), and 38.1 cm (15 in), each at an angle of 45 degrees to the ground. A bentonite layer was applied at the surface to avoid preferential flow paths (Product #0922W050, SoilMoisture Equipment Corporation, United States). Cup samplers were placed 20 cm apart in a horizontal line about one meter from the throughfall sampler, away from major roots or large trees. A suction of 80 psi was applied to each cup sampler on a weekly basis using a vacuum hand pump (Model 2005G2, SoilMoisture Equipment Corporation, United

States). Cup water samples (N=44) were extracted with a 1L polypropylene Erlenmeyer flask (1/8" O.D.) and nylon tubing and stopper assembly (3/32" O.D. and 1/4" O.D., respectively), suction was applied by hand pump until all the water in the cup sampler was drained into the flask.

3.3. Soil water content, temperature, and electrical conductivity sensors installation and monitoring

Soil conditions were monitored using a solar-powered HOBOlink Micro RX wireless data logger station (1-hr transmission interval) connected to three wireless HOBOnet T12 Soil Moisture (m^3/m^3)/Temperature (°C)/EC (dS/cm) sensors, each installed at 0 cm, 17.8 cm (7 in), and 38.1 cm (15 in) soil depth.

3.4. Soil physical and chemical analysis

Soil samples (N=116) were gathered from the surface down to 76.2 cm (30 in) in 12.7 cm (5 in) increments. Each sample was divided to fill two 1L size plastic bags and mailed to the Texas A&M AgriLife Extension Soil, Water and Forage Testing Laboratory for textural analysis (sand, silt, and clay content), organic matter content, pH, conductivity, nitrate-N, and nutrient levels testing. All analyses were reported on a dry soil basis.

Upon arrival at the Texas A&M soil testing laboratory, samples were transferred to an aluminum pan and oven-dried at 65°C (±2°C) in a forced air oven for 16 hours or until fully dry (Texas A&M AgriLife Extension Service, 2012). Samples were pulverized using an open mesh bottom hammer-style soil pulverizer and screened to remove particles larger than 2 mm. A weight loss-on-ignition procedure determined organic carbon, inorganic carbon, and total nitrogen (Schulte & Hopkins, 1996) after being ground to pass through a No. 80 mesh. Soil texture fractions were determined via a classical hydrometer

procedure (Day, 1965). In addition, soil was mixed with deionized water at a 1:2 ratio (Schofield & Taylor, 1955). Samples were stirred and allowed to sit for 30 minutes. A hydrogen-selective electrode was used to determine pH, and a conductivity probe was used to determine electrical conductivity in µmho/cm (Rhoades, 1982). Soil nitrate-N analysis was performed using a 10:1 ratio of 1 M KCl (Kachurina, et al., 2000) to pulverized soil sample. Before filtration through a Whatman #2 filter, 2g of the soil was placed into an extraction cup and agitated on a 200 rpm, 1-inch throw orbital shaker for 5 minutes. Samples were then analyzed by cadmium reduction (Kachurina et al., 2000). Phosphorous, potassium, calcium, magnesium, sulfur, and sodium were extracted from the soil using Mehlich III extractant, a dilute acid-fluoride-EDTA solution composed of 0.2N NH_4Cl-0.2N HOAc-0.015N NH_4F-0.012N HCl at approximately pH 2.5 (Mehlich, 1984). Soil nutrients were measured and identified by inductively coupled plasma spectroscopy.

3.5. Species selection

The aim of our selection of plants for this study was to include woody plant species common to the urban green landscape of the DFW metroplex. The following trees were selected for sampling: Elderberry (*Sambucus canadensis)*, Cherry laurel (*Prunus caroliniana)*, and Boxelder maple (*Acer negundo). S. canadensis* is a deciduous tree or shrub native to North America with a shallow but aggressive root system (NC State, 2024). The individual sampled was approximately 2.5 meters tall and bloomed white flowers at the end of April 2023. It had thin (up to 1cm diameter) fibrous roots at about 5cm depth in addition to the taproot. *P. caroliniana* is an evergreen tree native to the southern United States with a shallow but complex root system, making it drought-tolerant

when established (NC State, 2024). The sampled individual was approximately 9 meters tall and had roots within 10 to 30 cm of soil depth about 6 cm in diameter. Although the flower bloom time of this tree is in spring (University of Arizona, 2024), no flowers or fruit were observed throughout the year. *A. negundo* is a relatively short-lived (about 60 years; USDA, 2024), brittle-wooded, deciduous tree native to North America with shallow, strong lateral roots (NC State, 2024). The sampled individual was about 20 meters tall and had roots 1.57 m long (up to 5cm in diameter) at about 12 cm depth.

3.6. Stem and soil sample collection

Stem (N=166) and destructive soil (N=117) samples were collected during monthly campaigns throughout 2023 (February-December) and January of 2024. Samples were collected by cutting and removing woody stems. Twigs, leaves, and knots were removed. The branch was then trimmed and divided into six subsamples using 50-mL polypropylene conical centrifuge tubes (Falcon No. 352070) per species. Each centrifuge tube was filled on average with 30.4 g (stems) and 77.4 g (soils). Since our study aims to analyze the mobile water stored in the tree, the bark, phloem, and cambium layers of the stems were scraped off using a pocketknife, leaving only the xylem wood for extraction. Soil samples were collected in triplicates at 0 cm (surface), 12.7 cm (5 in), 25.4 cm (10 in), and 38.1 cm (15 in) using trench and handheld shovels. All centrifuge tubes were immediately covered with Parafilm, stored in a cooler with ice gel packs (5°C), and transported to the laboratory for water extractions. In the lab, samples were stored at approximately 5°C, and extractions were conducted within 1-2 days after collection.

3.7. Stem and soil water extraction and gravimetric analysis

Following the methodology proposed by Sánchez-Murillo et al. (2023), water was extracted from stem and soil samples via centrifugation (Eppendorf 5810R centrifuge) at 11,000 rpm and 5°C for 1.5 hours. Before centrifugation, all samples were weighed (wet mass) (±0.01 g) in the laboratory. Stem or soil material was removed to balance the masses in the centrifugation tubes. After centrifugation, the extracted water was transferred with a 1,000 microliter micro-pipettor (Four E's Scientific, United States) to a 2 mL glass vial and sealed with a septa cap. A 300 µL glass insert was used when the extracted water volume was below 1.0 mL. The remnant stem and plant samples were weighed (wet mass after centrifugation), transferred to an oven-safe aluminum pan, and oven-dried for 48 hours at 105°C. The final sample mass (oven-dried) was also recorded. Stem and soil water extracted (in %; extracted water/total water in the sample) and total stem and soil water (in %; total water in the sample/total sample mass) were calculated via gravimetric measurements.

3.8. Isotopic analysis

Isotopic analysis was conducted by the Tracer Hydrology Group in the Department of Earth and Environmental Sciences at the University of Texas-Arlington, using a GLA431-TLWIA triple water isotope analyzer. Three calibrated secondary standards 5D (δ^2H=−10.5‰, $\delta^{18}O$=−3.00‰, and $\delta^{17}O$=−1.52‰), 4D (δ^2H=−48.7‰, $\delta^{17}O$=−7.63‰, and $\delta^{18}O$=−3.97‰), and 1D (δ^2H=−161.3‰, $\delta^{18}O$=−20.72‰, and $\delta^{17}O$=−10.93‰) were used to normalize the results using a block standardization procedure (i.e., LGR LWIA Post Analysis Software Version 4.5.0.6). An additional standard was used as an internal con-

trol, IC ($\delta^{2}H$=−78.0‰, $\delta^{17}O$=−10.76‰, and $\delta^{18}O$=−5.63‰). This internal control was injected three times per analytical batch. The total number of injections per sample or standard comprised two preparation and eight measure injections. The $^{18}O/^{16}O$ and $^{2}H/^{1}H$ ratios are presented in delta notation δ (‰), relative to the VSMOW2-SLAP2 scale. The analytical uncertainty was ±0.33‰ for $\delta^{2}H$ and ±0.08 ‰ for $\delta^{18}O$. The deuterium excess (hereafter *d*-excess; Dansgaard, 1954) was calculated as *d*-excess= $\delta^{2}H-8\times\delta^{18}O$. The LC-excess (Landwehr & Coplen, 2006) was computed as LC-excess = $\delta^{2}H = a\times\delta^{18}O-b$, where a and b are the slope and intercept of the meteoric water line, respectively.

3.9. Bayesian Mixing Model

The R package *simmr* (Parnell and Inger, 2016) was used to evaluate the mean contribution (±1σ) of water source endmembers to a mixture following Sánchez-Murillo et al. (2023). This assessment aimed to understand from which soil depth each plant primarily sourced water during the growing season (spring 2023). Two isotope compositions were used for the mixing modeling: $\delta^{18}O$ (‰) and *d*-excess (‰) (as a proxy of evaporation). Several assumptions and conditions guided mixing calculations: i) the extracted plant water was treated as a representative mixture of the water stored in the plant xylem, ii) each soil depth was treated as a single endmember (0, 12.7, 25.4, and 38.1 cm), iii) soil depths were determined based on textural analysis and known root profiles for the plant species; iv) we expected minimal impacts of the extraction method on plant water source estimations due to sufficiently large isotopic differences among endmembers, negligible extraction amount-effect, and low values of organic contamination via centrifugation.

Chapter 4: Results

4.1. Weather, soil water content, soil temperature, and textural characteristics

4.1.1 Precipitation and air temperature

The total precipitation amount in the Fort Worth area (Figure 2) during the study period (January 2023 to March 2024) was 888.0 mm. The total precipitation per season during this period was as follows: 143.8 mm (winter 2023), 132.3 mm (spring 2023), 38.4 mm (summer 2023), 125.5 mm (fall 2023), and 227.3 mm (winter 2024) (Figure 2). The mean annual air temperature in the study area was 19.1°C from January 2023 to March 2024, with a mean summer temperature of 31.9°C and mean winter temperatures of 11.6°C and 9.7°C during 2023 and 2024, respectively. The minimum winter temperature was -8.9°C (winter 2024), and the maximum summer temperature was 35.8°C (summer 2023). Mean air temperatures were 22.1°C in spring 2023 and 17.3°C in fall 2023 (Figure 2).

4.1.2 Soil water content and temperature seasonal changes

The mean soil water content (SWC) was close to field capacity (FC) for clay loam and loam soils at all depths: 0.26±0.08 m^3/m^3 (0cm), 0.27±0.06 m^3/m^3 (17.8cm), and 0.26±0.06 m^3/m^3, and (38.1cm) (USDA, 2019) (Figure 2). However, large SWC changes were observed within seasons at all depths. At the surface, SWC was close to the wilting point (WP) during summer (0.11 m^3/m^3), whereas SWC was between FC and WP between 17.8 cm and 38.1 cm (0.18-0.26 m^3/m^3) during summer. Saturated SWC averaged 0.37 m^3/m^3 during rainy periods (spring, fall, and winter). Mean soil temperature was 19.5°C throughout the soil column. Higher soil temperatures were recorded at the surface during summer (32.1°C) compared to deeper soil layers (30°C at 17.8 cm and

29.4°C at 38.1 cm). During winter, the minimum soil temperature changed from 2.2°C (0cm) to 7.1°C (38.1 cm) (Figure 2).

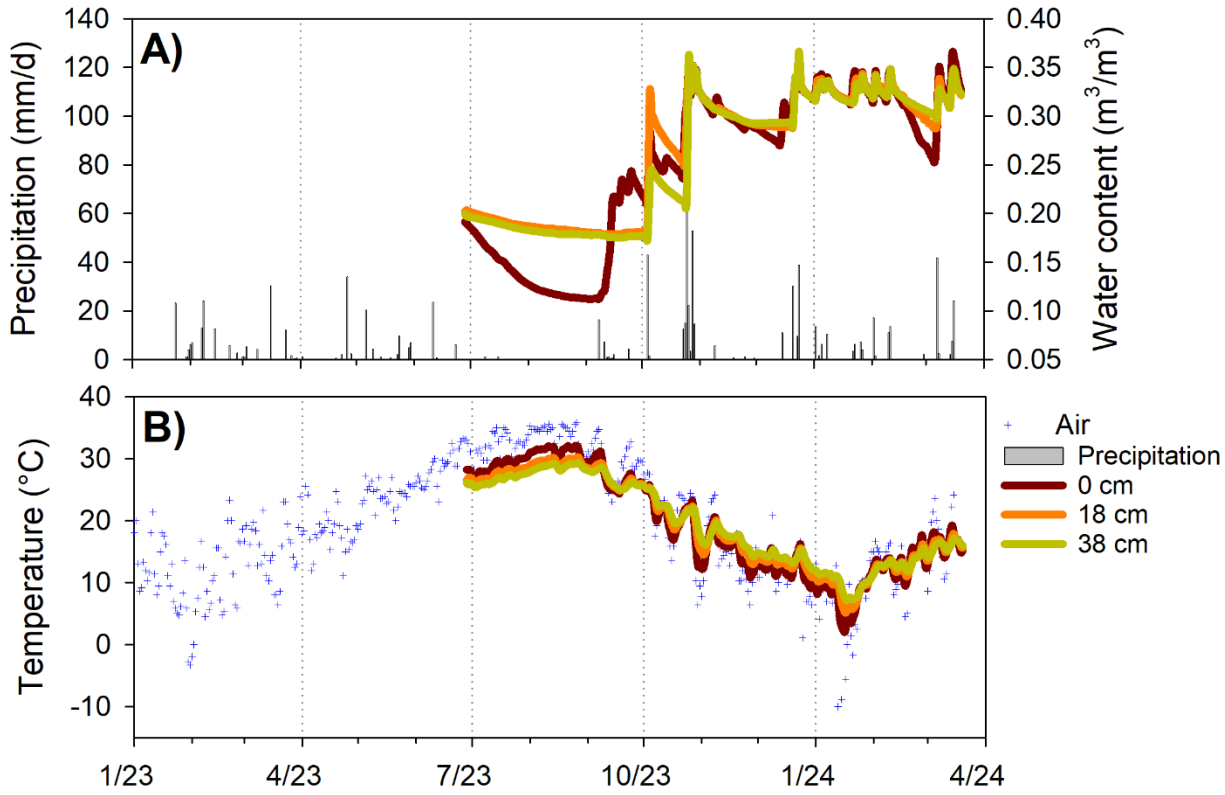

Figure 2: *A) Precipitation (mm/d) and soil water content (m^3/m^3) at three depths (0, 18, 38 cm). B) Mean daily air and soil temperature at three depths (0, 18, 38 cm).*

4.1.3 Soil texture

The textural class of the soils ranged from loam at the surface (0cm) to clay loam at all other depths sampled (12.7cm, 25.4cm, and 38.1cm), with increasing clay content with depth. Clay content was 26%, 28%, 33%, and 34% at depths of 0cm, 12.7cm, 25.4cm, and 38.1cm, respectively. The sand contents of each depth were 39% (0cm), 40% (12.7cm), 25% (25.4cm), and 23% (38.1cm). The proportions of silt for each depth

were 35% (0cm), 32% (12.7cm), 42% (25.4cm), and 43% (38.1cm). Organic matter content decreased with depth as follows: 8.20% (0cm), 4.05% (12.7cm), 2.63% (25.4cm), and 2.30% (38.1cm).

4.2. Soil and plant total water content and water extracted

The proportion of water extracted via centrifugation and the sample total water content (calculated by gravimetric analysis) were used to examine the potential effects of extracted water volume on soil and stem isotope values. Figures (3 and 4) show the total water (%) and extracted water (%) in the stem and soil samples, respectively. Overall, water was extracted from 69.5% and 78.5% of stem and soil samples.

The mean total water content of destructive soil samples was 26.87±7.53%. Surface layers exhibited the greatest total water content at 37.39±6.35% (0 cm) and 24.53±3.66% (12.7 cm). At greater depths of 25.4 cm and 38.1 cm, total water content was more uniform (22.67±.365% and 22.63±2.61%). Mean total water content for all soil depths was greatest during the spring, except for soils at 25.4 cm depth, which showed the greatest total water content during winter 2024. While most soil depths showed uniform values (~20%), there was an increase in variability of surface (0 cm) soil mean water content during the fall (34.08±5.68%) (Figure 3). These values are in agreement with the volumetric SWC.

The mean total water content of the stems was 51.41±11.80%. Boxelder Maple exhibited a mean total water content of 47.07±5.34% with large seasonal variability (11.3% to 64.62%) (Figure 3). Cherry Laurel exhibited a mean total water content of 42.36±3.21%, with slightly lower values of 39.24±1.46% and 39.37±1.23% in winter 2023 and summer, respectively. Cherry Laurel stems showed their highest mean total water

content during the fall (45.89±4.70%), along with their greatest variability. Cherry Laurel had no new living stems for sampling in winter 2024. Elderberry exhibited a mean total water content of 61.73±13.25%, with higher values in the spring (73.54±11.28%) and lower values in winter 2024 (11.41±0.06). Elderberry total water content displayed the highest variability among all stems (Figure 3).

Of the three stem endmembers, water was extracted from 80.3% of Boxelder Maple samples, 52.1% of Cherry Laurel samples, and 72.7% of Elderberry samples. The mean extracted water from the stems was 6.83±4.76%. Boxelder Maple exhibited the greatest mean extracted water (8.57±4.56%), while Cherry Laurel showed the lowest (2.96±1.67%) (Figur 4). Boxelder Maple stems mean extracted water values were highest and most variable during the spring (11.24±4.94%), with more uniform values during winter 2023 (5.69±3.23%), summer (7.28±3.94%), and fall (9.96±3.76%). No water was extracted from Boxelder Maple stems during the winter of 2024. Cherry Laurel stems mean extracted water values were highest and most variable in the fall (5.09±2.51), with the lowest values and variation during winter 2023 (1.87±0.65%) (Figure 4). Elderberry mean extracted water values (6.72±4.14%) decreased from winter 2023 (9.08±3.67%) to fall (3.33±1.99%), with the highest variability during the spring (6.75±4.68). No water was extracted from Elderberry stem samples in the winter of 2024 (Figure 4).

Soil water was extracted from all samples at different depths as follows: 75.0% (0 cm), 79.3% (12.7 cm), 84.6% (25.4 cm), and 75.9% (38.1cm). The mean extracted water from the soils was 12.8±7.3%. During the summer, water was extracted from only one soil sample at 0 cm depth (15% water content). Mean extracted water was highest for surface layers at 0 cm (14.71±7.46%) and 12.7 cm (13.73±5.75%). Mean extracted water

of deeper soil layers was 12.74±6.94% (25.4 cm) and 9.88±8.16% (38.1 cm). The mean extracted water was highest during winter 2023 at 0cm and 12.7cm, whereas the highest values were observed during winter 2024 at 25.4cm and 28.1cm. The lowest soil water extracted values were recorded during fall for all soil depths, except at 38.1 cm depth (lowest during spring) (Figure 4).

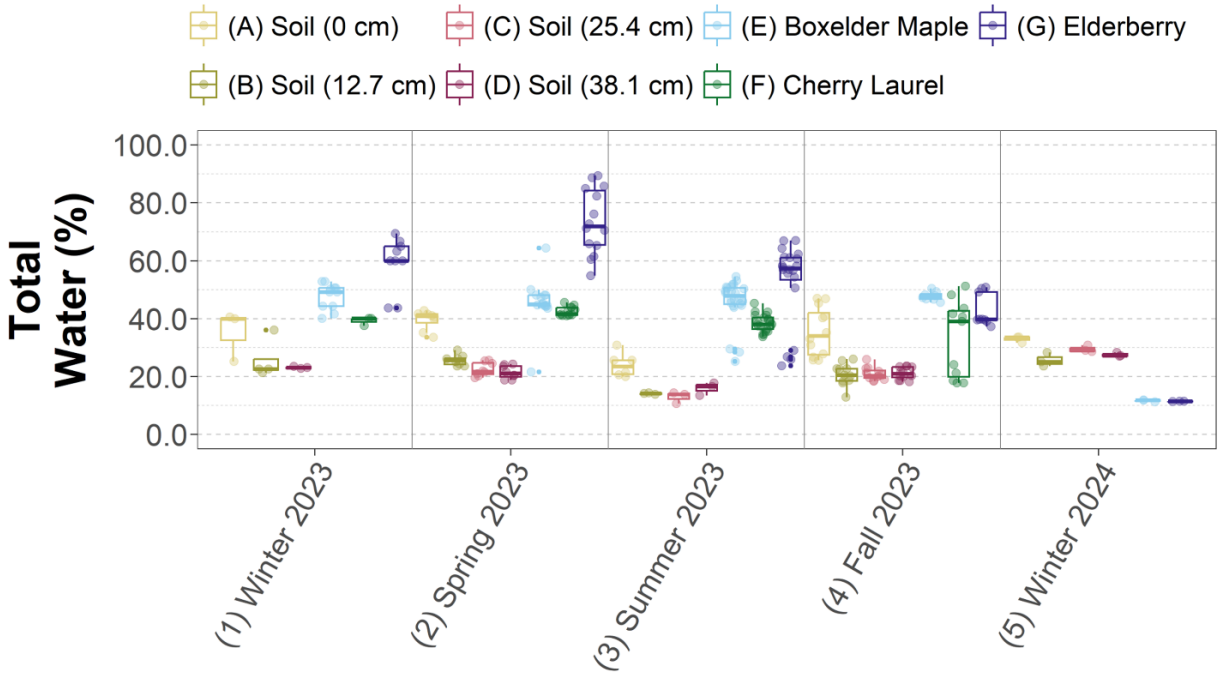

***Figure 3**: Seasonal box plots for sample total water content (%) for each soil depth and three selected urban plant species.*

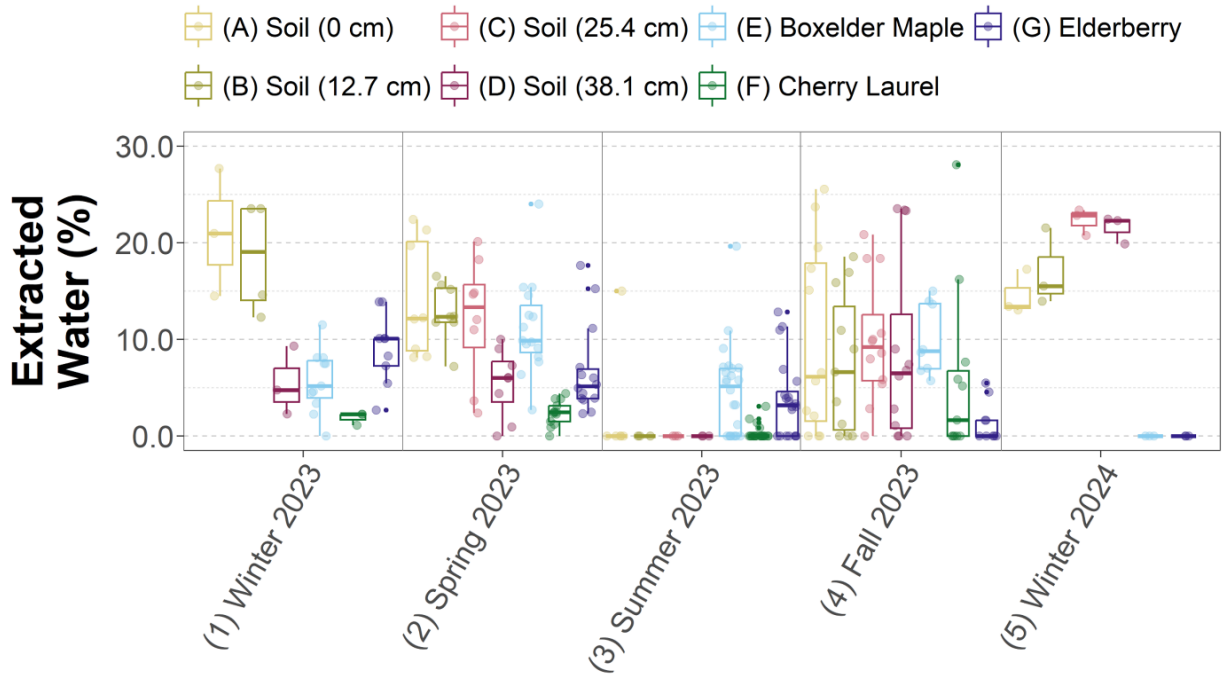

Figure 4: *Seasonal box plots for centrifuged extracted water (%) for each soil depth and three selected urban plant species.*

4.3. Extracted amount-effect on stem and soil isotopic compositions

Overall, mean water extracted volumes ranged from ~100 µL to 7.5 mL in stem samples and from ~100 µL to 10.5 mL in soil samples. A linear regression analysis was conducted to examine the effects of extracted water amount on isotope values. No significant water amount-dependent relationships (with $\delta^{18}O$ or *d*-excess) were detected in the stem and soil isotope values (Figure 5). A previous study using centrifugation to extract water from soils and stems in five different tropical ecosystems also reported negligible influence of the water extraction amount on the resulting isotopic compositions (Sánchez-Murillo et al., 2023).

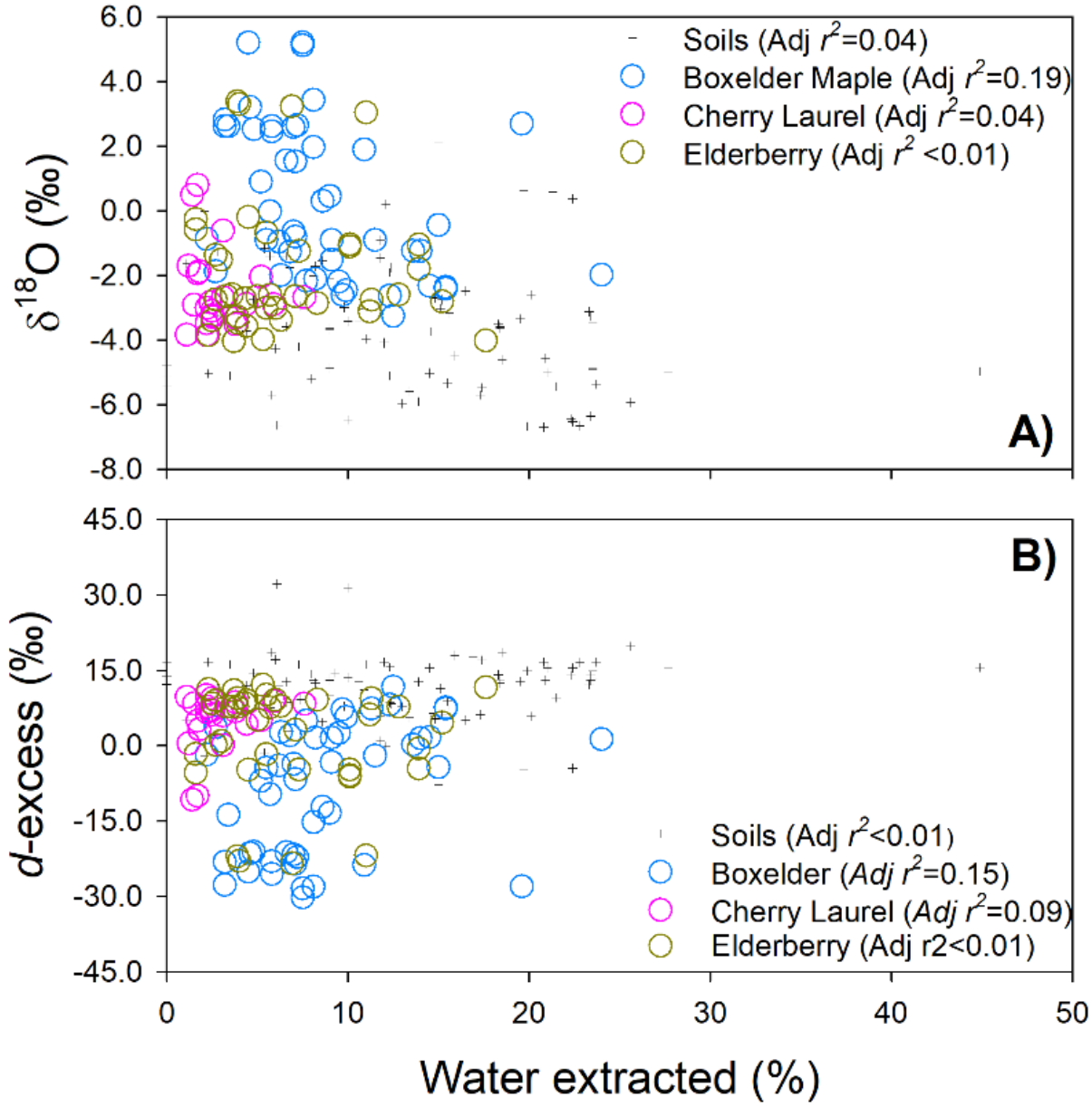

Figure 5: *Relationship between centrifugated extracted water (%), $\delta^{18}O$ (‰), and d-excess (‰) composition for soils and plants (Bolxelder Maple, Cherry Laurel, and Elderberry). Adjusted R^2 values denote the insignificant influence of the extracted water amount on the isotopic compositions.*

4.4. Narrowband metric and broadband metric distribution

The narrowband metric represents organic contamination within the extracted water (e.g., methanol) (Brian Leen et al., 2012). Narrowband values (unitless) ranged overall from 0.04 to 2.08 (mean 0.23±0.40) (Figure 6). For reference, the mean narrowband metric values of the throughfall and soils (considered not contaminated) were 0.04±0.01 and 0.05±0.01, respectively. Water extracted from Boxelder Maple exhibited the highest mean narrowband values (0.34±0.49) and ranged from 0.05 to 2.02 (median=0.08). Elderberry showed a mean narrowband value of 0.16±0.33, ranging from 0.05 to 2.08 (median=0.08). Cherry Laurel had a mean narrowband value of 0.11±0.06, ranging from 0.04 to 0.25 (median=0.09). These low median values are in the reported range of methanol concentrations below 25 ppm_v, corresponding to potential isotope measurement errors below 0.2% in $\delta^{18}O$ and $\delta^{2}H$ (Brian Leen et al., 2012) (Figure 6).

The broadband metric represents organic contamination with alcohols such as ethanol. Broadband values overall ranged from 0.99 to 1.07 (throughfall and soil broadband values both were 1.00±0.00). Boxelder Maple exhibited a mean broadband value of 1.00±0.02, ranging from 1.00 to 1.07 (median=1.00). Elderberry had a mean broadband value of 1.00±0.01, ranging from 1.00 to 1.04 (median=1.00). Cherry showed a mean broadband value of 1.00±0.00, ranging from 0.99 to 1.00 (median=1.00) (Figure 6). Broadband values showed virtually no dispersion across all extracted water samples. These broadband values also represent the minimal influence of large organic molecules with -OH groups (Brian Leen et al., 2012).

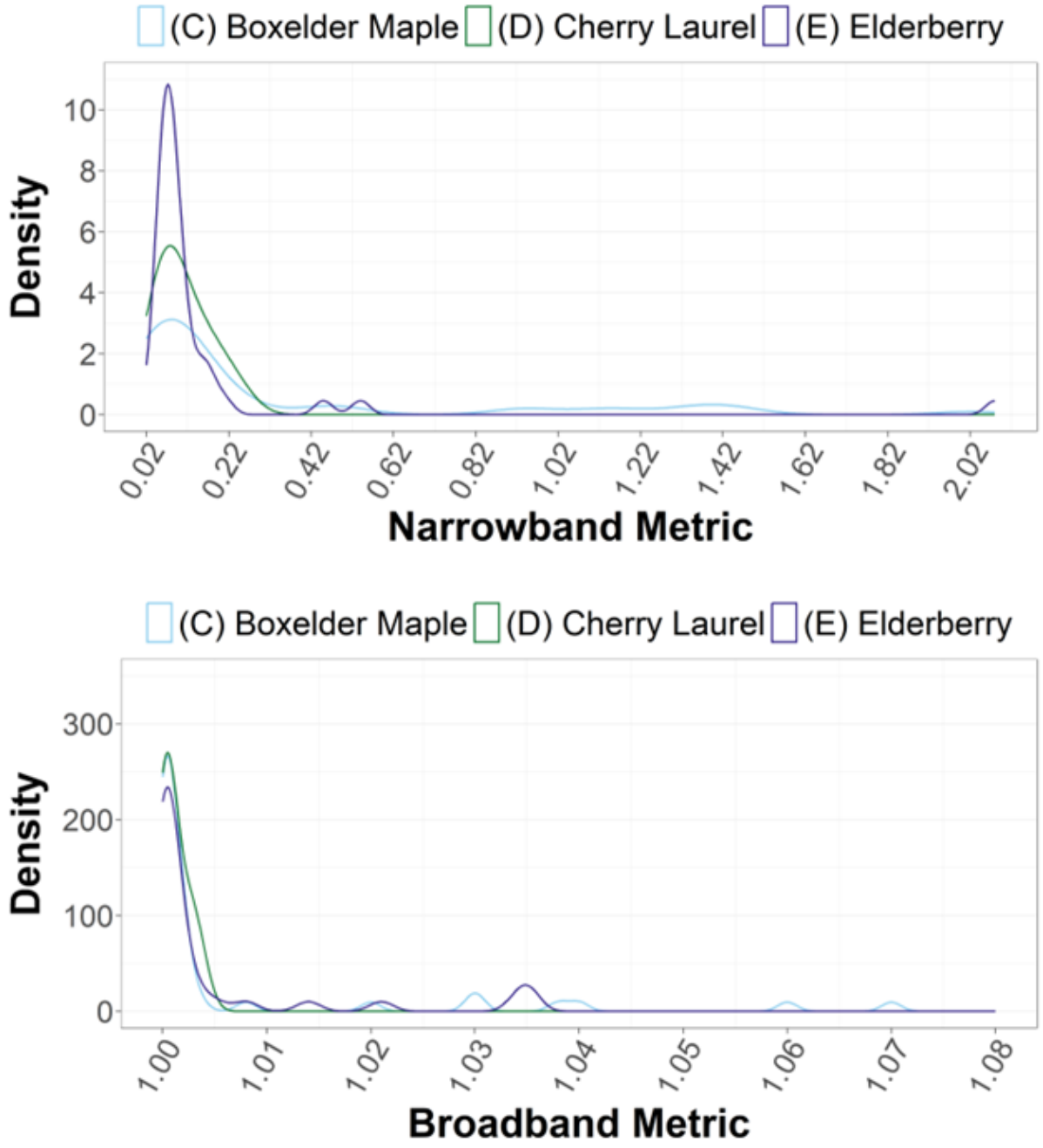

Figure 6: *Narrowband (upper panel) and broadband (bottom panel) metric density distributions in all stem water samples analyzed.*

4.5. Stem and soil seasonal variability

Boxelder Maple ($\delta^{18}O$ mean=0.29±2.43‰) showed progressively depleted $\delta^{18}O$ values from winter 2023 (+2.74±2.26‰) to fall 2023 (-0.51±0.71‰) (Figure 7). Cherry Laurel ($\delta^{18}O$ mean= -2.47±1.26‰) displayed the most uniform values of all stem samples, ranging from -3.84‰ to +0.80‰. Stem water from this tree experienced a slight enrichment from -3.72±0.21‰ in winter 2023 to -0.98±1.15‰ in the summer, followed by a slight depletion in the fall (-1.70±1.71‰) (Figure 7). Of all the trees sampled, Cherry Laurel also showed the most connectivity to throughfall (-1.42‰) during the summer 2023 water-stressed season, with a mean $\delta^{18}O$ value of -0.98±1.15‰. Elderberry showed enrichment from winter 2023 (-1.76±0.86‰) to spring 2023 (-0.48±2.79‰). Relatively enriched Elderberry $\delta^{18}O$ values in the summer (-0.48±2.79‰) were accompanied by a rise in variability, with a range of -2.75‰ to +3.38‰ (Figure 7). Similar trends were observed for $\delta^{2}H$ due to the high collinearity between $\delta^{18}O$ and $\delta^{2}H$ (Figure 8).

Soils experienced increasing variability with depth during the winter 2023 season. These values agree with the winter 2023 throughfall ($\delta^{18}O$ mean= -4.40±2.06‰) input (Figure 7). During the spring, soils showed steady depletion with depth, with mean $\delta^{18}O$ values of -0.58±1.30‰ (0cm), -2.21±0.70‰ (12.7cm), -3.35±0.83‰ (25.4cm), and -3.38±0.83‰ (38.1cm). During summer, water from only one soil sample of 0 cm depth was extracted, with an enriched value of +2.14‰. Similar to the winter season, values were comparable to one another across all depths during the fall, ranging from -2.97‰ to -4.34‰. However, surface soil water exhibited much higher variability in the fall (-5.92‰ to -0.02‰) than in the winter (-7.10‰ to 3.34‰) (Figure 7).

4.5.1. Winter (2023)

Winter 2023 mean soil $\delta^{18}O$ values (-4.03±0.86‰) agreed with throughfall (-4.40±2.06‰) inputs and became more enriched with depth. The mean $\delta^{18}O$ values of the soils were as follows: -4.59±0.83‰ (0cm), -3.96±0.81‰ (12.7cm), -4.20±0.49‰ (25.4cm), and -3.50±1.12‰ (38.1cm). Winter 2023 mean soil *d*-excess values (+14.00±2.84‰) were uniform and matched throughfall (+14.00±6.08‰) (Figure 9). Boxelder Maple showed strong enrichment in $\delta^{18}O$ (+2.74±2.26‰) compared to the soils and had the lowest mean *d*-excess (-18.14±10.79‰) of the plants during this season. Cherry Laurel $\delta^{18}O$ (-3.72±0.21‰) agreed with $\delta^{18}O$ values (-3.96±0.81‰) at 12.7cm soil. Cherry Laurel had a *d*-excess value of +9.18±1.22‰ (Figure 9). Elderberry $\delta^{18}O$ (-1.76±0.86‰) and *d*-excess (+0.20±7.12‰) values showed a strong deviation from soils (Figures 7 and 9).

4.5.2. Spring (2023)

The spring growing season presented the most uniform isotope ratios, with $\delta^{18}O$ ranging from -6.62‰ to +0.62‰. Mean soil $\delta^{18}O$ values (-2.99±1.56‰) became more depleted with depth: -0.58±1.30‰ (0cm), -2.21±0.70‰ (12.7cm), -3.35±0.83‰ (25.4cm), and -3.38±0.83‰ (38.1cm). Throughfall mean $\delta^{18}O$ was -2.83±1.57‰. Deeper soils (25.4cm and 38.1cm) were more depleted in $\delta^{18}O$ than recent throughfall inputs and matched previous winter 2023 values apart from a slight enrichment (Figure 8). Soil *d*-excess values increased with depth (+3.40±9.8‰ at 0cm to +18.1±7.29‰ at 38.1cm). Boxelder Maple $\delta^{18}O$ values (-2.30±0.42‰) corresponded with throughfall, shallow soils, and 25.4cm soils, while Cherry Laurel $\delta^{18}O$ (-2.95±0.84‰) and Elderberry (-3.37±0.49‰) concurred with throughfall and deeper soils (25.4cm). Plant mean *d*-excess values were:

Boxelder Maple (+5.00±3.16‰), Cherry Laurel (+6.46±2.43‰), and Elderberry (+8.30±2.76‰) (Figure 9).

4.5.3. Summer (2023)

Water was extracted from only one soil sample (0cm) during the summer of 2023, with a $\delta^{18}O$ value of +2.14‰ and *d*-excess of -7.73‰ (Figures 8 and 10). Surface soil was more enriched in the summer than in any other season and had more enriched $\delta^{18}O$ values than the throughfall (-1.42±1.48‰). Boxelder $\delta^{18}O$ values (+1.50±1.54‰) agreed with the soil, but *d*-excess (-18.57±9.01‰) values were more negative than the throughfall. Cherry Laurel $\delta^{18}O$ (-0.98±1.15‰) values matched the throughfall more than the other plants during this season. Cherry Laurel *d*-excess was (-0.61±7.03‰). Elderberry had diverse $\delta^{18}O$ values (-0.48±2.79‰), ranging from -2.75‰ to +3.38‰ and agreeing with both throughfall and soil (Figures 7 and 9).

4.5.4. Fall (2023)

During fall 2023, mean soil $\delta^{18}O$ (-3.40±1.53‰) values showed a response to throughfall inputs (-4.22±1.89‰). The mean $\delta^{18}O$ values at each depth were as follows: -2.97±1.95‰ (0cm), -4.34±0.75‰ (12.7cm), -3.34±1.58‰ (25.4cm), and -3.15±1.34‰ (38.1cm). The overall soil $\delta^{18}O$ variability was highest during this season, ranging from -5.92‰ to -0.02‰. Boxelder Maple (-0.51±0.71‰) and Elderberry (-0.42±0.24‰) were enriched in $\delta^{18}O$, showing values disconnected from any soil depths or throughfall sampled. Boxelder Maple exhibited a lower mean *d*-excess (-4.91±6.15‰) than throughfall (+14.00±6.32‰) and soils (+11.48±5.12‰), while Elderberry exhibited the lowest *d*-excess (-3.36±1.98‰) during this season. Cherry Laurel $\delta^{18}O$ values (-

1.70±1.71‰) were similar to shallow soil sources. Cherry Laurel had the highest mean *d*-excess (+3.10±8.85‰) value of the plants during fall 2023 (Figures 7 and 9).

4.5.5. Winter (2024)

No water was extracted from the stems during the winter of 2024. Throughfall was the most depleted in $\delta^{18}O$ (-7.61±0.40) compared to previous seasons. Soils $\delta^{18}O$ values (-5.96±0.97‰) agreed with throughfall, with shallow soil water showing higher $\delta^{18}O$ values (0cm; -6.08±0.70‰) than deeper soils (38.1cm; -6.54±0.12‰). Deuterium excess increased with depth (+10.14±7.28‰ at 0cm to +14.81±0.73‰ at 38.1cm) (Figures 7 and 9).

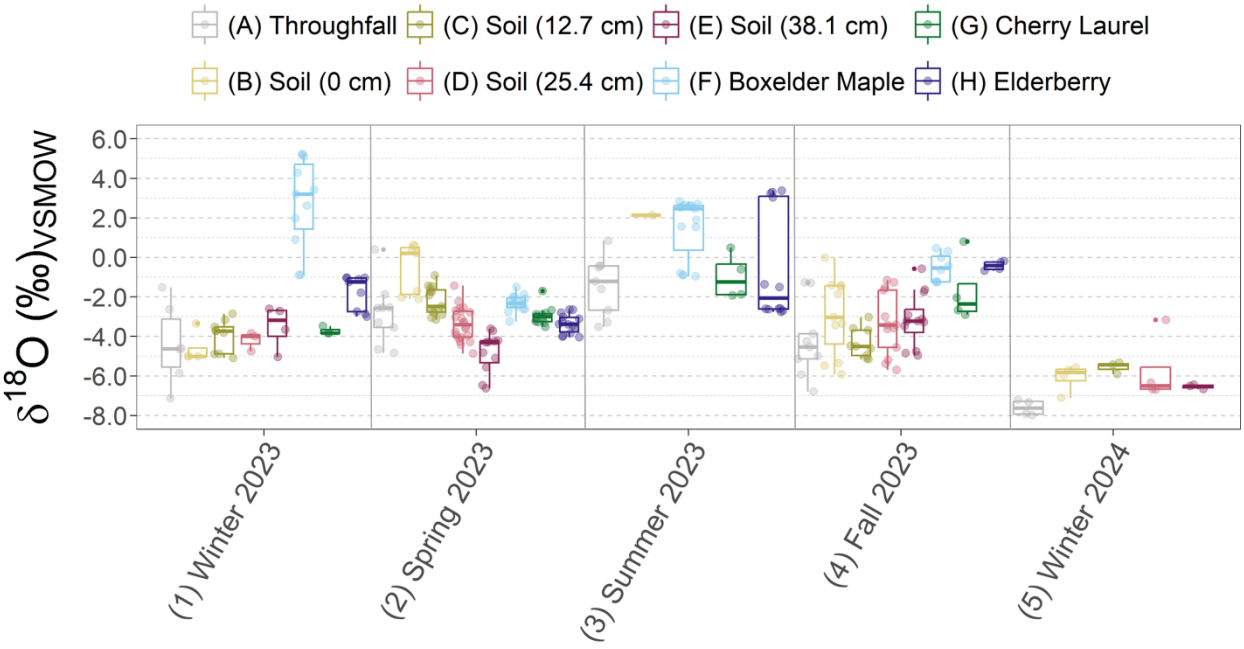

Figure 7: *Box plots show seasonal $\delta^{18}O$ (‰) variability of throughfall, soil water (per depth), and xylem water (2023-2024).*

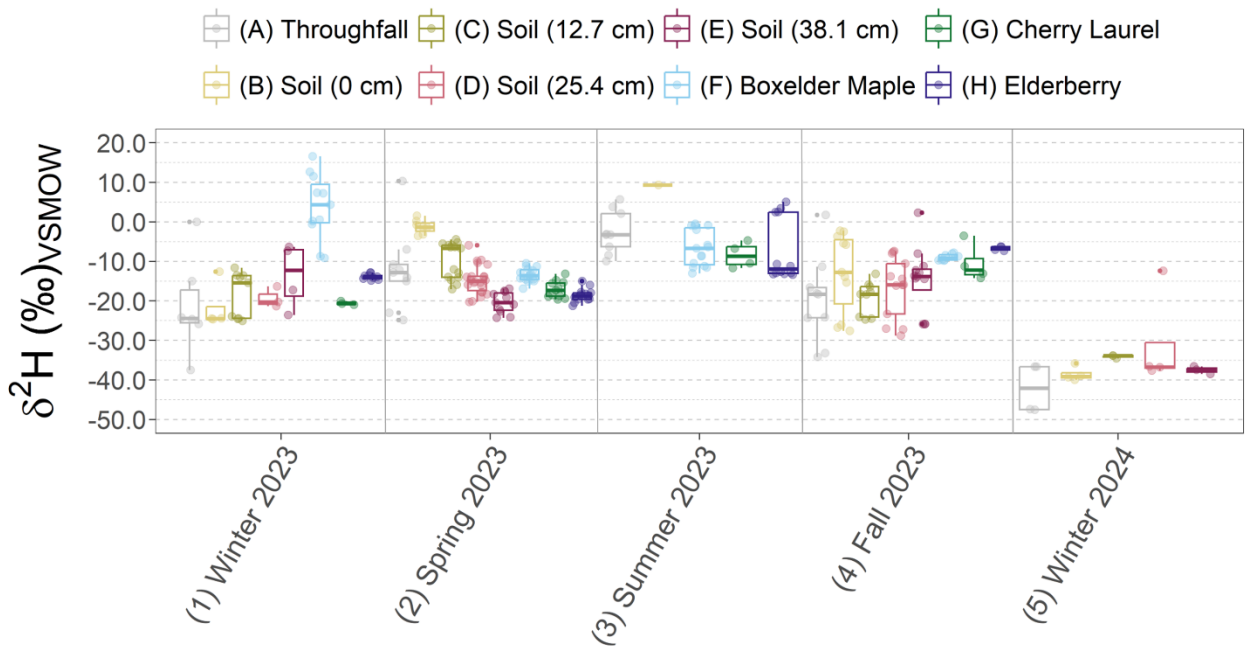

Figure 8: *Box plots showing seasonal δ2H (‰) variability of throughfall, soil water (per depth), and xylem water (2023-2024).*

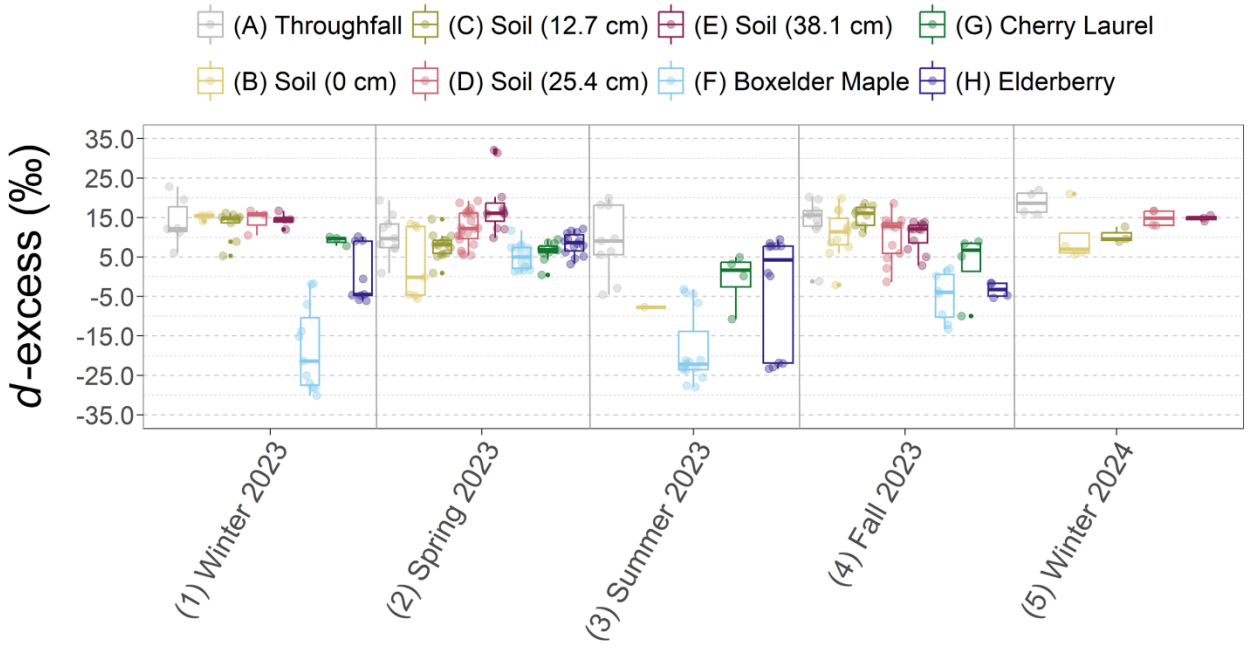

Figure 9: *Box plots showing seasonal d-excess (‰) variability of throughfall, soil water (per depth), and xylem water (2023-2024).*

4.5.6. LC-excess variability

Boxelder Maple and Elderberry were disconnected from Arlington regional precipitation during winter 2023 (LMWL: $\delta^2H = 5.97 \cdot \delta^{18}O + 6.66$; R^2=0.88 and N=34). Mean *LC*-excess of Boxelder Maple (-19.23±6.51‰) showed the strongest deviations from local meteoric conditions (Figure 10). Elderberry (-10.08±5.38‰) also showed more negative values compared to the throughfall (-1.59±4.09‰) and soils (-0.83±2.61‰). Cherry Laurel (-5.02±0.81‰), however, showed the lease deviation from regional precipitation.

In spring 2023 (LMWL: $\delta^2H = 5.95 \cdot \delta^{18}O + 6.09$; R^2=0.80 and N=105), plants, throughfall, and soils more closely resembled regional precipitation. Throughfall mean LC-excess values (-1.42±4.28‰) agreed with soil (-1.08±4.37‰) and were more positive than Boxelder Maple (-5.79±2.47‰), Cherry Laurel (-5.67±1.66), and Elderberry (-4.66±1.86‰) values.

LC-excess values represented a disconnection of the plants from the regional precipitation for the remainder of 2023. During summer 2023 (LMWL: $\delta^2H = 5.33 \cdot \delta^{18}O + 2.88$; R^2=0.83 and N=35), throughfall (+2.15±5.62‰) showed positive mean *LC*-excess with Boxelder Maple (-17.46±5.22‰) and Elderberry (-7.54±7.03‰) showing much lower values. The singular soil water sample (0cm; -4.91‰) and Cherry Laurel (-6.10±4.19%) mean *LC*-excess showed the most similarity to precipitation other than throughfall.

In fall 2023 (LMWL: $\delta^2H = 7.14 \cdot \delta^{18}O + 13.71$; R^2=0.91 and N=131), *LC*-excess of throughfall was negative (-3.36±5.19), and values decreased with soil depth (-5.42±4.49‰ (0cm) to -5.89±2.89‰ (38.1cm)). Boxelder Maple (-19.05±5.53‰) and

Elderberry (-17.43±1.78‰) still showed much more negative values, and Cherry Laurel (-12.08±7.38‰) exhibited a stronger divergence than in summer.

Finally, in winter 2024 (LMWL: $\delta^2H = 8.48 \cdot \delta^{18}O + 16.92$; R^2=0.91 and N=50), throughfall (+5.50±2.92‰) *LC*-excess had positive values, while soil values showed an increase and greater connectivity to precipitation with depth (-3.87±7.61‰ (0cm) to +1.04±0.75‰ (38.1cm).

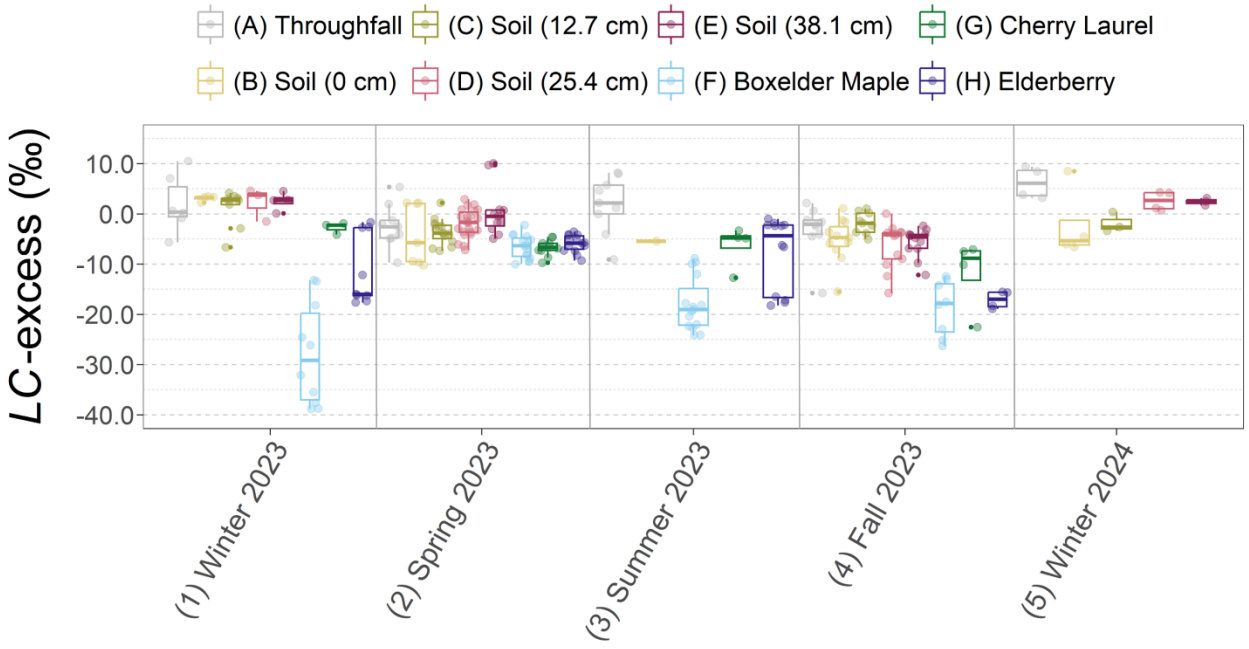

Figure 10: *Box plots showing seasonal LC-excess (‰) variability of throughfall, soil water (per depth), and xylem water (2023-2024).*

4.6. Dual-isotope space and narrow band variations

Figures 11-13 show the dual isotope plots (Arlington LMWL: $\delta^2H = 7.42 \cdot \delta^{18}O + 10.04$; R^2=0.93 and N=498) per plant, including throughfall, soils, and stems characterized by season (shape) and degree of organic contamination or narrowband

metric (size). The narrowband metric was used here due to the wider metric distribution. Overall, throughfall and soil narrowband exhibited a mean value of 0.05±0.01 and varied from 0.03 to 0.08.

Boxelder Maple ($\delta^2H = 2.87 \cdot \delta^{18}O - 7.56$; R^2=0.79 and N=49) exhibited the lowest slope and intercept, showing the strongest deviations from meteoric conditions. These deviations mainly occurred during winter 2023, summer 2023, and fall 2023. Boxelder Maple narrowband metrics reached maximums of 1.45 and 2.02 during summer and fall, respectively (Figure 11). The most enriched isotope values in Boxelder Maple occurred in winter 2023, during which the maximum narrowband metric value was 0.19. Cherry Laurel ($\delta^2H = 3.78 \cdot \delta^{18}O - 5.49$; R^2=0.88 and N=22) exhibited the highest slope and intercept of the plants and aligned strongly with soil and throughfall isotopic compositions. The maximum narrowband value was 0.25, occurring during the fall 2023 sampling campaign (Figure 12). Elderberry's ($\delta^2H = 3.15 \cdot \delta^{18}O - 7.10$; R^2=0.91 and N=39) most enriched values occurred in summer, during which the maximum narrowband value was 0.12. During the spring, Elderberry showed its overall maximum narrowband value of 2.08, which corresponded with the week of its bloom (Figure 13).

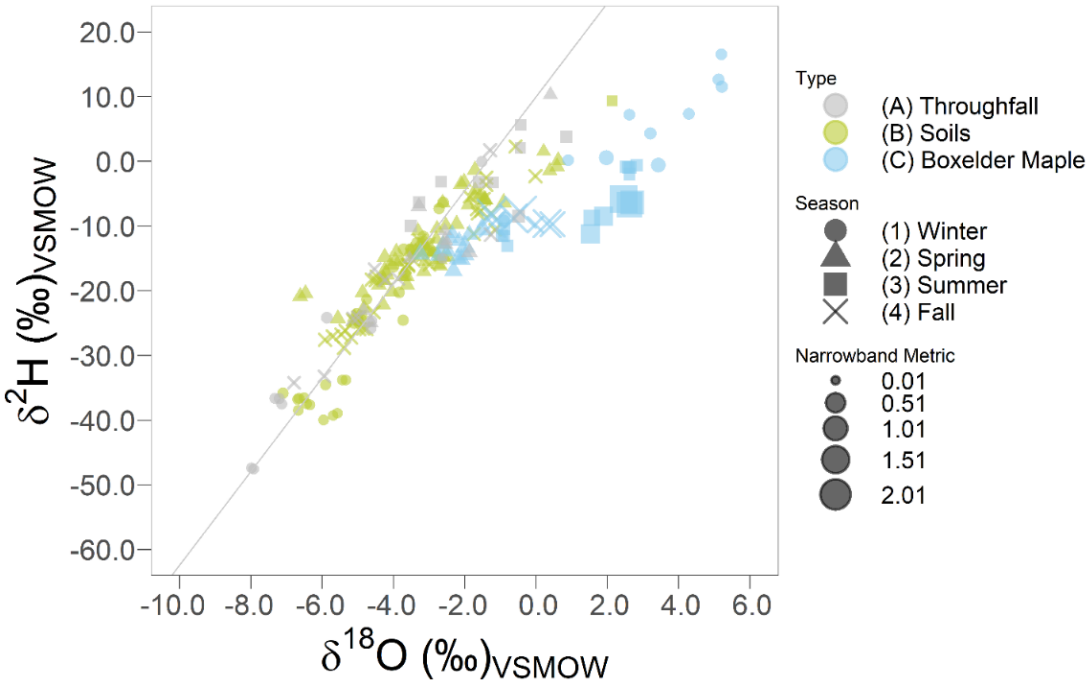

***Figure 11**: Dual isotope plot showing throughfall, soils, and Boxelder Maple isotopic and narrowband variability via centrifugation.*

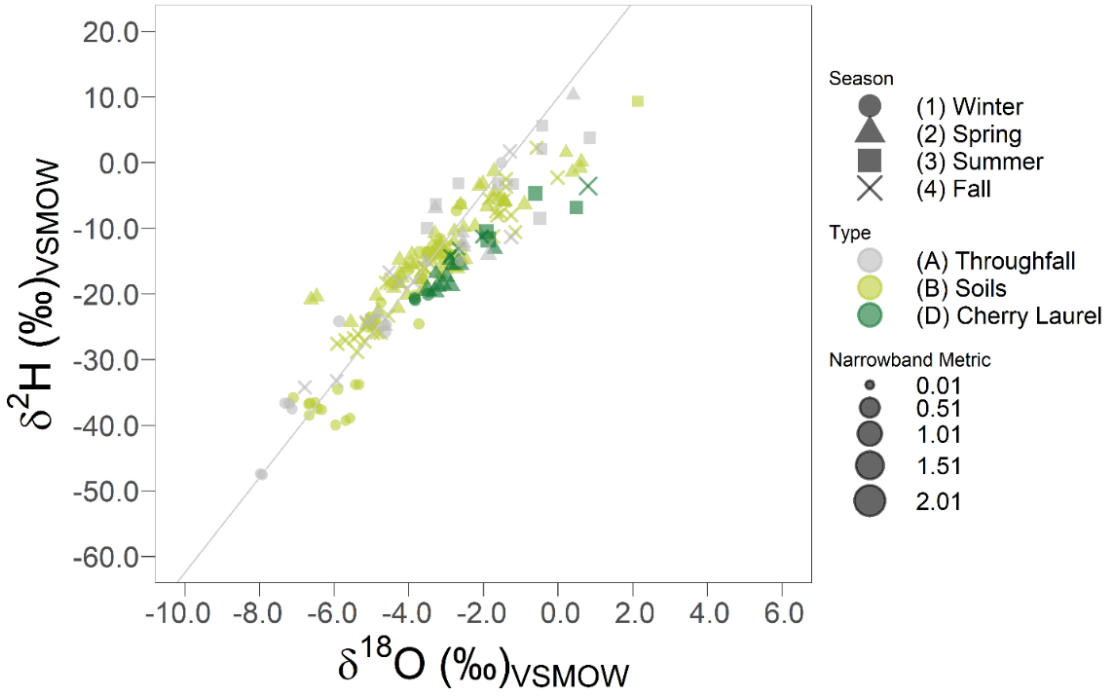

Figure 12*: Dual isotope plot showing throughfall, soils, and Cherry Laurel isotopic and narrowband variability via centrifugation.*

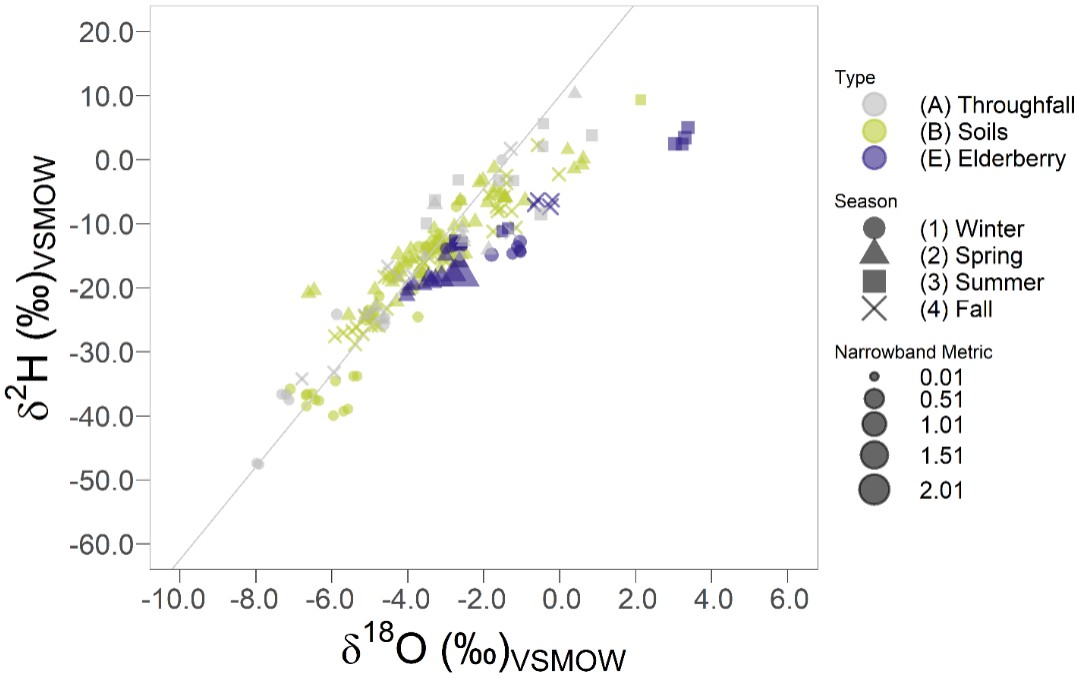

Figure 13: *Dual isotope plot showing throughfall, soils, and Elderberry isotopic and narrowband variability via centrifugation.*

4.7. Bayesian Mixing Analysis

Figure 14 shows the source contribution (%) of each soil depth to the water found in the plant stems during spring 2023 (active growing season). Boxelder Maple showed source water contributions mainly from 12.7cm soils (52.1%). The other contributions were 23.7% (0cm), 14.1% (25.4cm), and 7.70% (38.1cm). Cherry Laurel mixtures also showed source water contributions mainly from 12.7cm soils (41.3%). The other contributions were 15.3% (0cm), 24.0% (25.4cm), and 14.6% (38.1cm). Elderberry mixtures showed source water contributions mainly from 25.4cm soils (33.2%). Other contributions were 10.5% (0cm), 29.9% (12.7cm), and 22.2% (38.1cm). In summary, the most important soil water sources were shallow soil (0cm and 12.7cm) for Boxelder

Maple, shallow to deep soil (12.7cm and 25.4cm) for Cherry Laurel, and deep soil (25.4cm and 38.1cm) for Elderberry.

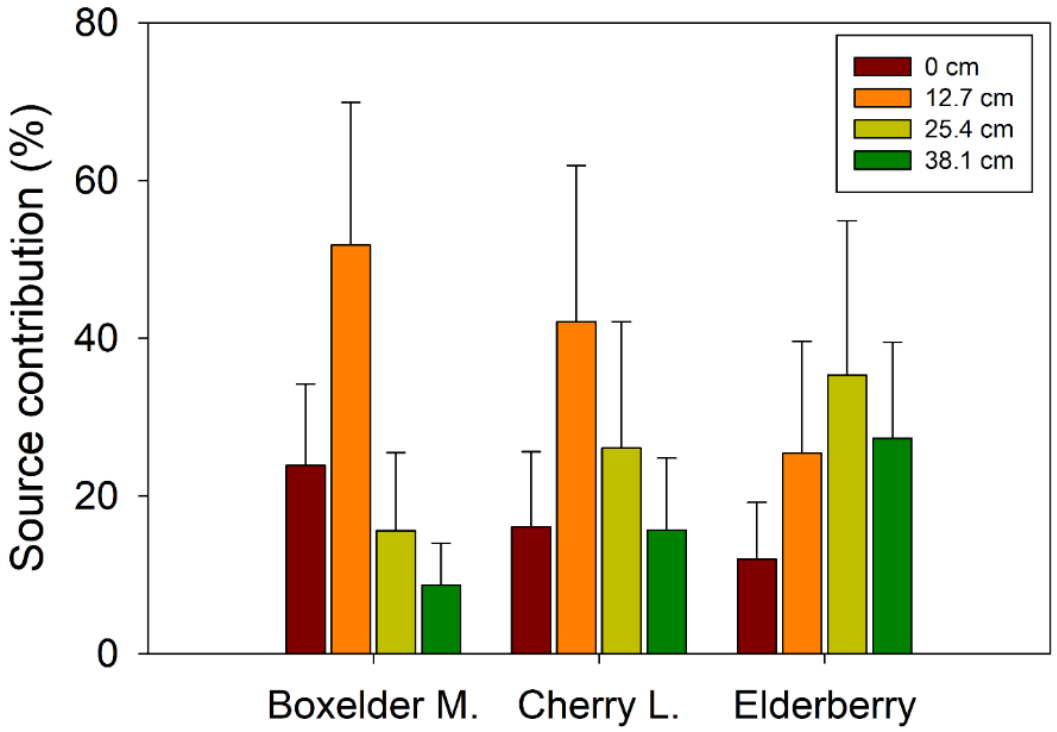

***Figure 14**: Source contribution proportions of soil water from 0cm, 12.7cm, 25.4cm, and 38.1cm depths to Boxelder Maple, Cherry Laurel, and Elderberry mixtures during spring 2023.*

Chapter 5: Discussion

While cryogenic vacuum distillation is an effective method that results in high extraction success rates (Wen et al., 2022), it may also extract a combination of mobile water and chemically bound water (i.e., bounded water to the soil minerals and plant tissue and not a part of the urban water cycling or source water flowing through the plant) (von Freyberg et al., 2020). Isotope values obtained from this combination of mobile and immobile water may contain a deuterium bias (Duvert et al., 2024; Chen et al., 2020) and not reflect the 'true' water which is taken up and involved in evapotranspiration. In contrast, the centrifugation method for extracting water from soils and live woody plants has been shown to extract mobile water effectively, even during drier seasons when the water content of plants and soils is lower (Sánchez-Murillo et al., 2023). Cavitron, a method of water extraction similar to centrifugation but which applies centrifugal force to the stem attached to a rotor fitted to a centrifuge (rather than placing the stem into a tube onto which the centrifugal force is applied), has also been compared by Barbeta et al. (2022) to cryogenic methods. They found that the xylem water extracted by the cavitron represented the source water more closely than bulk stem (xylem, phloem, and all other plant tissue) water extracted via the cryogenic method. Our centrifugation method showed a high success rate with no amount-dependent effect on the isotope values (i.e., artificially depleted or enriched values). Overall, the centrifugation method appears to be an accessible, straightforward, and relatively cost-effective process to obtain water for source partition analysis of plants from a plethora of samples in a short amount of time.

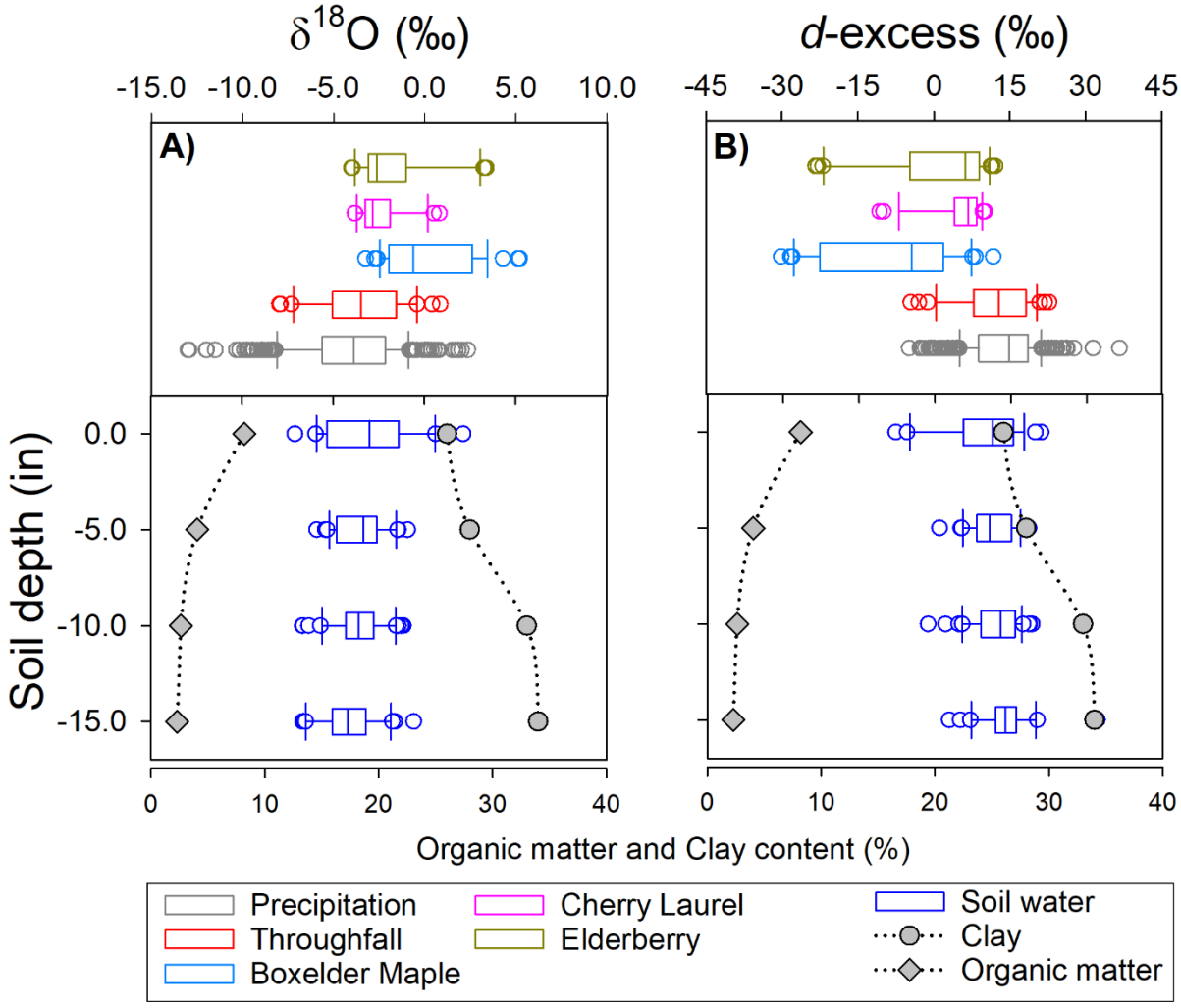

Figure 15: *Summary plot including $\delta^{18}O$ and d-excess variability of soil water, precipitation (2022-2024), throughfall (2023-2024), xylem, and soil water (2023-2024). This plot also shows the organic matter and clay content (%) of the soils (0cm to 38.1cm).*

Millar et al. (2021) found that organic contamination caused significant errors in stable isotope analysis by laser spectroscopy. However, our results indicated that deviations from meteoric conditions or soil water are not correlated with high levels of organic contamination (i.e., narrowband metric). The highest narrowband values in Boxelder Maple occurred in summer 2023, during which the tree's extracted water

percent was lowest. It is possible that these high narrowband values were due to a ‘dilution effect’; since there was less water present in the stems, the organic contamination became more prevalent. High narrowband metrics occurring in the fall suggest a lag time between the mixing of new water with the summer stored water. However, Cherry Laurel consistently had the lowest total water content (drier stems) and showed no significantly high narrowband metric values or deviations from meteoric conditions. Elderberry’s only high narrowband value can be explained by its flowering during late spring, which involves higher production of sugars and organic acids (Veberic, 2009) in the sap flow. This study did not reveal unreliable isotope ratios caused by organic contamination.

The water uptake preferences of urban tree species in the DFW metropolitan area have not been widely studied amid increasing urban development. Urban vegetation can lower outdoor air temperatures in urban heat islands, reduce energy use, improve air quality, and decrease stormwater runoff and floods (California Air Resources Board, 2024). Our results show a one-year long observation of the diverse water use strategies of three trees in a highly altered urban environment. Overall, Cherry Laurel and Boxelder Maple isotope values corresponded to shallow soil water sources, while Elderberry favored deeper soil water (Figure 15). Soil isotopic variability decreased with depth, implying less influence of surface evaporation.

The three trees we sampled each have differing water uptake strategies that shift with the seasons (i.e., changes in temperature, precipitation, and soil moisture). Here, we focus on the spring active growing season. Water extracted from Boxelder Maple agreed with shallow soil water sources and lateral and extended root profile, indicating an

opportunistic quick uptake of new rainfall. This species is short-lived and fast-growing and is recommended for quick growth in urban riparian plantings (USDA, 2024). Isotope values matching those of 12.7cm and 25.4cm soil water show Cherry Laurel's preference for slightly deeper water sources. Surprisingly, the much more shrub-like Elderberry showed a significant preference for deep soil water (25.4cm and 38.1cm) during the spring season, suggesting that the tap root (vertical profile) contributed the most to the water transport process during the flowering season. The uptake of deep soils suggest that this plant may better tolerate occasional droughts (UNH, 2024).

Drought tolerant plants are often used in landscape architecture in water-scarce areas, and water-conserving landscaping is a commonly used solution to preserving green spaces in urban areas despite climate change. About 25% of the urban water supply is used to water landscapes and gardens, and xeric plants can reduce landscape water use by over 50% (Özyavuz and Özyavuz, 2012). However, trees are not commonly considered parts of xeric landscape design. This can result in a landscape that is visually appealing but lacks shade and complex taproot systems, which prevent soil erosion in cohesive soils (Vannoppen et al., 2017). The study and discovery of the drought tolerance of tree species can facilitate the selection of trees for green spaces in water-limited environments with clayey soils. Furthermore, the study of tree species' unique water uptake strategies, i.e., their preferred source water depth, can aid in irrigation planning that conserves water by targeting the depth of maximum uptake potential by the specific plant.

Chapter 6: Conclusions

Our results provide evidence of the effectiveness of using the centrifugation method for water extraction from stems and soils in a subtropical urban landscape with high clay content (up to 34%). Overall, this technique resulted in a successful extraction rate of 69.5% and 78.5% for all the stem and soil samples collected throughout a hydrological year. In addition, our extraction protocol allows water isotope laser measurements with minimal organic interference and no extraction-amount effects. This study also contributes to the knowledge of plant water uptake strategies of three common urban tree species in the DFW area, an environment that experiences flashy stormwater episodes that can cause flooding. Our findings indicate distinct soil water uptake depths, ranging from shallow (Boxelder Maple and Cherry Laurel) to deeper soil layers (Elderberry). Future studies should include isotopic analysis of soils (spatial heterogeneity), stems from multiple individuals of the same species, and sap flow measurements to determine the time of highest evapotranspiration activity. These results may be used to inform city planners and designers on incorporating specific plants into the evolving urban landscape as a component of sustainable development.

References

1. Allen, S. T. and Kirchner, J. W. (2022). Potential effects of cryogenic extraction biases on plant water source partitioning inferred from xylem-water isotope ratios. *Hydrological Processes, 36*(2), e14483. doi: 10.1002/hyp.14483
2. Barbedo, J., Miguez, M., Van Der Horst, D., and Marins, M. (2014). Enhancing ecosystem services for flood mitigation: a conservation strategy for peri-urban landscapes?. *Ecology and Society, 19*(2), 54. http://dx.doi.org/10.5751/ES-06482-190254
3. Barbeta, A., Burlett, R., Martín-Gómez, P., Fréjaville, B., Devert, N., Wingate, L., et al. (2022). Evidence for distinct isotopic compositions of sap and tissue water in tree stems: consequences for plant water source identification. *New Phytologist, 233*(3), 1121-1132. https://doi.org/10.1111/nph.17857
4. Best, B. (2021, September 13). The BRIT prairie. *Fort Worth Botanic Garden*. https://fwbg.org/research-projects/biodiversity-and-floristics/the-brit-prairie/
5. Brian Leen, J., Berman, E. S., Liebson, L., and Gupta, M. (2012). Spectral contaminant identifier for off-axis integrated cavity output spectroscopy measurements of liquid water isotopes. *Review of Scientific Instruments, 83*(4). https://doi.org/10.1063/1.4704843
6. Ceperley, N., Gimeno, T. E., Jacobs, S. R., Beyer, M., Dubbert, M., Fischer, B., and Rothfuss, Y. (2024). Toward a common methodological framework for the sampling, extraction, and isotopic analysis of water in the Critical Zone to study vegetation water use. *Wiley Interdisciplinary Reviews: Water*, e1727. https://doi.org/10.1002/wat2.1727

7. Chen Y., Helliker B. R, Tang X., Li F., Zhou Y., Song X. (2020). Stem water cryogenic extraction biases estimation in deuterium isotope composition of plant source water. *Proceedings of the National Academy of Sciences, 117*(52), 33345-50. https://doi.org/10.1073/pnas.2014422117
8. California Air Resources Board. (2024). Benefits of Urban Vegetation. *Cool California*; State of California. https://coolcalifornia.arb.ca.gov/benefits-of-urban-vegetation
9. Dalton, F. N. (1989). Plant root water extraction studies using stable isotopes. In: *Structural and Functional Aspects of Transport in Roots Developments in Plant and Soil Sciences*, eds B. C. Loughamn, O. Gašparíková, and J. Kolek (Dordrecht: Springer), pp. 151–155. doi: 10.1007/978-94-009-0891-8_29
10. Day, P. R. (1965). Particle fractionation and particle-size analysis. In: C. A. Black, et al. (ed.). *Methods of Soil Analysis: Part 1. Agronomy Monogr.* (p.545-567) ASA and SSSA, Madison, WI.
11. Duvert, C., Barbeta, A., Hutley, L. B., Rodriguez, L., Irvine, D. J., and Taylor, A. R. (2024). Cavitron extraction of xylem water suggests cryogenic extraction biases vary across species but are independent of tree water stress. *Hydrological Processes, 38*(2), e15099. https://doi.org/10.1002/hyp.15099
12. El-Shenawy, M. I., Herwartz, D., and Staubwasser, M. (2024). A passive method for sampling water in the soil–plant–atmosphere continuum for stable hydrogen and oxygen isotope analyses. *Rapid Communications in Mass Spectrometry, 38*(2), e9646. https://doi.org/10.1002/rcm.9646

13. Fischer, B., Frentress, J., Manzoni, S., Cousins, S.A., Hugelius, G., Greger, M., Smittenberg, R.H. and Lyon, S.W. (2019). Mojito, anyone? An exploration of low-tech plant water extraction methods for isotopic analysis using locally-sourced materials. *Frontiers in Earth Science, 7,* p.150. https://doi.org/10.3389/feart.2019.00150
14. Gaj, M., Kaufhold, S., Koeniger, P., Beyer, M., Weiler, M., and Himmelsbach, T. (2017) Mineral mediated isotope fractionation of soil water. *Rapid Commun. Mass Spectrom.,* doi: 10.1002/rcm.7787.
15. Geris, J., Tetzlaff, D., McDonnell, J., Anderson, J., Paton, G. and Soulsby, C. (2015). Ecohydrological separation in wet, low energy northern environments? A preliminary assessment using different soil water extraction techniques. *Hydrological Processes, 29*(25), 5139-5152. DOI: 10.1002/hyp.10603
16. Gralher, B., Herbstritt, B., and Weiler, M. (2021). Unresolved aspects of the direct vapor equilibration method for stable isotope analysis (δ 18 O, δ 2 H) of matrix-bound water: unifying protocols through empirical and mathematical scrutiny. *Hydrology and Earth System Sciences, 25*(9), 5219-5235. https://doi.org/10.5194/hess-25-5219-2021
17. Green, D., O'Donnell, E., Johnson, M., Slater, L., Thorne, C., Zheng, S., ... and Boothroyd, R. J. (2021). Green infrastructure: The future of urban flood risk management?. *Wiley Interdisciplinary Reviews: Water, 8*(6), e1560. https://doi.org/10.1002/wat2.1560
18. Griffith, G. E., Bryce, S. A., Omernik, J. M., Comstock, J. A., Rogers, A. C., Harrison, B., Hatch, S. L., and Bezanson, D. (2004) Ecoregions of Texas (color poster

with map, descriptive text, and photographs): Reston, Virginia, U.S. Geological Survey (map scale 1:2,500,000)

19. Gröning, M., Lutz, H. O., Roller-Lutz, Z., Kralik, M., Gourcy, L., and Pöltenstein, L. (2012). A simple rain collector preventing water re-evaporation dedicated for Δ18O and Δ2H analysis of cumulative precipitation samples. *Journal of Hydrology*, *448–449*, 195–200. https://doi.org/10.1016/j.jhydrol.2012.04.041
20. He, D., Wen, M., Wang, Y., Du, G., Zhang, C., He, H., Jin, J., Li, M., and Si, B. (2023). Xylem Water Cryogenic Vacuum Extraction: Testing Correction Methods with CaviTron-Based Apple Twig Sampling. *Journal of Hydrology, 621*, 129572. https://doi.org/10.1016/j.jhydrol.2023.129572
21. Herbstritt, B., Gralher, B., Seeger, S., Rinderer, M., and Weiler, M. (2023). Technical note: Discrete in situ vapor sampling for subsequent lab-based water stable isotope analysis, *Hydrol. Earth Syst. Sci., 27,* 3701–3718, https://doi.org/10.5194/hess-27-3701-2023, 2023.
22. Jusserand, C. (1980). Extraction de l'eau interstitielle des sédiments et dessols—Comparaison des valeurs de l'oxygène 18 par différentes méth-odes, premiers résultats. *Catena. 7*(1), 87–96. https://doi.org/10.1016/S0341-8162(80)80006-3
23. Kachurina, O. M., H. Zhang, W. R. Raun, and E. G. Krenzer. (2000). Simultaneous determination of soil aluminum, ammonium- and nitrate-nitrogen using 1 M potassium chloride extraction. *Commun. Soil Sci. and Pl. Anal. 31*, 893-903.
24. Koeniger, P., Marshall, J. D., Link, T., and Mulch, A. (2011). An inexpensive, fast, and reliable method for vacuum extraction of soil and plant water for stable isotope

analyses by mass spectrometry. *Rapid Communications in Mass Spectrometry. 25*(20), 3041–3048.https://doi.org/10.1002/rcm.5198

25. Landwehr, J. M., and Coplen, T. B. (2006). Line-conditioned excess: A new method for characterizing stable hydrogen and oxygen isotope ratios in hydrologic systems. In *Isotopes in Environmental Studies*, 1st ed., IAEA-CN-118/56:(pp.132-135). IAEA. https://inis.iaea.org/search/search.aspx?orig_q=RN:37043527.
26. Lourenço, I. B., de Oliveira, A. K. B., Marques, L. S., Barbosa, A. A. Q., Veról, A. P., Magalhães, P. C., and Miguez, M. G. (2020). A framework to support flood prevention and mitigation in the landscape and urban planning process regarding water dynamics. *Journal of Cleaner Production, 277*, 122983. https://doi.org/10.1016/j.jclepro.2020.122983
27. Mehlich, A. (1984). Mehlich-3 soil test extractant: a modification of Mehlich-2 extractant. *Commun. Soil Sci. Plant Anal. 15*(12), 1409-1416. https://doi.org/10.1080/00103628409367568
28. Millar, C., Janzen, K., Nehemy, M. F., Koehler, G., Hervé-Fernandez, P., McDonnell, JJ. (2021). Organic contamination detection for isotopic analysis of water by laser spectroscopy. *Rapid Commun Mass Spectrom, 35*(15), e9118. https://doi.org/10.1002/rcm.9118
29. Millar, C., Janzen, K., Nehemy, M. F., Koehler, G., Hervé-Fernández, P., Wang, H., Orlowski, N., Barbeta, A., and McDonnell, J. J. (2022). On the urgent need for standardization in isotope-based ecohydrological investigations. *Hydrological Processes, 36*(10), e14698. https://doi.org/10.1002/hyp.14698

30. National Centers for Environmental Information (NCEI). (2024). Daily summaries station details. Daily Summaries Station Details: FORT WORTH NAS, TX US, GHCND:USW00013911, Climate Data Online (CDO)., *National Climatic Data Center (NCDC)*. https://www.ncdc.noaa.gov/cdo-web/datasets/GHCND/stations/GHCND:USW00013911/detail
31. North Carolina State University. (2024). Acer negundo. *North Carolina Extension Gardener Plant Toolbox.* https://plants.ces.ncsu.edu/plants/acer-negundo/ ; Prunus caroliniana. https://plants.ces.ncsu.edu/plants/prunus-caroliniana/ ; Sambucus canadensis. https://plants.ces.ncsu.edu/plants/sambucus-canadensis/
32. Orlowski, N., Breuer, L., McDonnell, J. J. (2016). Critical issues with cryogenic extraction of soil water for stable isotope analysis. *Ecohydrology, 9*(1), 1-5. https://doi.org/10.1002/eco.1722
33. Orlowski, N., Frede, H. G., Brüggemann, N., and Breuer, L. (2013). Validation and application of a cryogenic vacuum extraction system for soil and plant water extraction for isotope analysis. *Journal of Sensors and Sensor Systems, 2*(2), pp.179-193. https://doi.org/10.5194/jsss-2-179-2013
34. Özyavuz, A and Özyavuz, M. (2012). Xeriscape in Landscape Design. In Özyavuz, M. (Ed.) *Landscape Planning,* (pp. 353-360). InTech. 10.5772/38989.
35. Parnell, A. C. and Inger, R. (2016). simmr: A stable isotope mixing model. R Package version 0.4.1.
36. Ping, Z.H., Nguyen, Q.T., Chen, S.M., Zhou, J.Q., and Ding, Y.D. (2001). States of water in different hydrophilic polymers-DSC and FTIR studies. Polymer 42 (2001) 8461-8467.

37. Renée Brooks, J., Barnard, H. R., Coulombe, R., and McDonnell, J. J. (2010). Ecohydrologic separation of water between trees and streams in a Mediterranean climate. *Nature Geoscience, 3*(2), 100-104. https://doi.org/10.1038/ngeo722

38. Rhoades, J. D. (1982). Soluble salts. In A. L. Page, et al. (ed.). *Methods of Soil Analysis: Part 2* (pp. 167-178). Agronomy Monogr. 9. 2nd ed. ASA and SSSA, Madison, WI.

39. Sánchez-Murillo, R., Esquivel-Hernández, G., Birkel, C., Correa, A., Welsh, K., Durán-Quesada, A. M., Sánchez-Gutiérrez, R. and Poca, M. (2020). Tracing water sources and fluxes in a dynamic tropical environment: from observations to modeling. *Frontiers in Earth Science, 8,* p.571477. https://doi.org/10.3389/feart.2020.571477

40. Sánchez-Murillo, R., Todini-Zicavo, D., Poca, M., Birkel, C., Esquivel-Hernández, G., Chavarría, M. M., Zuecco, G., and Penna, D. (2023). Dry season plant water sourcing in contrasting tropical ecosystems of Costa Rica. *Ecohydrology, 16*(5), e2541. https://doi.org/10.1002/eco.2541

41. Schulte, E. E. and B. G. Hopkins. (1996). Estimation of soil organic matter by weight Loss-On-Ignition. In F. R. Magdoff, M. A. Tabatabai and E. A. Hanlon, Jr. (Ed.), *Soil Organic matter: Analysis and Interpretation* (pp. 21-23). Special publication No. 46. Soil Sci. Soc. Amer. Madison, WI.

42. Schofield, R. K. and Taylor, A. W. (1955). The measurement of soil pH. *Soil Science Society of America. 19*, 164-167. https://doi.org/10.2136/sssaj1955.03615995001900020013x

43. Sobota, M., Li, K., Hren, M., and Knighton, J. (2024). Evidence for variations in cryogenic extraction deuterium biases of plant xylem water across foundational northeastern US trees. *Hydrological Processes, 38*(2), e15079. https://doi.org/10.1002/hyp.15079
44. Song, X., Chen, Y., Helliker, B. R., Tang, X., Li, F., and Zhou, Y. (2021). Reply to Evaristo et al.: Strong evidence for the need of correcting extraction bias in an early study of ecohydrological separation. *Proceedings of the National Academy of Sciences, 118*(17), p.e2103604118. doi: 10.1073/pnas.2103604118
45. Sprenger, M., Herbstritt, B., and Weiler, M. (2015). Established methods and new opportunities for pore water stable isotope analysis, *Hydrological Processes, 29,* 5174–5192, https://doi.org/10.1002/hyp.10643
46. Texas A&M AgriLife Extension. (2012, September). Soil, Water and Forage Testing Laboratory Methods. *Soil Testing Lab.* https://soiltesting.tamu.edu/laboratory-methods/
47. Texas A&M AgriLife Extension. (2024). Historic ETo Reference. *TexasET network.* https://texaset.tamu.edu/DataSummary/Daily/83
48. Texas Water Development Board. (2012). Chapter 4: Climate of Texas. In *Water for Texas 2012 State Water Plan* (pp. 145-147). Texas Water Development Board.
49. Thielemann, L., Gerjets, R., Dyckmans, J. (2019). Effects of soil-bound water exchange on the recovery of spike water by cryogenic water extraction. *Rapid Commun Mass Spectrom. 33*, 405– 410. https://doi.org/10.1002/rcm.8348
50. University of Arizona. (2022). Yavapai County Native & Naturalized Plants, *Acer negundo* - boxelder. *College of Agriculture, Life, and Environmental Sciences*.

https://cales.arizona.edu/yavapaiplants/SpeciesDetail.php?genus=Acer&species=negundo.

51. University of New Hampshire (2020). What is the best way to grow elderberries? *Ask UNH Extension.* https://extension.unh.edu/blog/2020/08/what-best-way-grow-elderberries

52. U.S. Department of Agriculture (2019). ROSETTA Class Average Hydraulic Parameters. *Agricultural Research Service.* https://www.ars.usda.gov/pacific-west-area/riverside-ca/agricultural-water-efficiency-and-salinity-research-unit/docs/model/rosetta-class-average-hydraulic-parameters/

53. U.S. Department of Agriculture NRCS National Plant Data Center & the Biota of North America Program. (2024). Plant guide: Boxelder (Acer negundo L.). *USDA Natural Resources Conservation Service.* https://plants.usda.gov/DocumentLibrary/plantguide/pdf/pg_acne2.pdf

54. U.S. Department of Commerce, NOAA. (2023, April 6). Dallas/Fort Worth Climate Narrative. *National Weather Service.* https://www.weather.gov/fwd/dfw_narrative

55. U.S. Department of Commerce, NOAA. (2024, January 17). DFW - normals, means, and extremes. *National Weather Service.* https://www.weather.gov/fwd/dfw_records_normals

56. Vannoppen, W., De Baets, S., Keeble, J., Dong, Y., Poesen, J. (2017). How do root and soil characteristics affect the erosion-reducing potential of plant species?. *Ecological Engineering, 109,* Part B, 186-195, ISSN 0925-8574, https://doi.org/10.1016/j.ecoleng.2017.08.001.

57. Veberic, R., Jakopic, J., Stampar, F., Schmitzer, V. (2009). European elderberry (Sambucus nigra L.) rich in sugars, organic acids, anthocyanins and selected polyphenols. *Food Chemistry, 114*(2), 511-515, ISSN 0308-8146, https://doi.org/10.1016/j.foodchem.2008.09.080

58. von Freyberg, J., Allen, S. T., Grossiord, C., Dawson, T. E. (2020). Plant and root-zone water isotopes are difficult to measure, explain, and predict: Some practical recommendations for determining plant water sources. *Methods Ecol Evol. 11*, 1352– 1367. https://doi.org/10.1111/2041-210X.13461

59. Wassenaar, L. I., Terzer-Wassmuth, S., Douence, C., Araguas-Araguas, L., Aggarwal, P. K., Coplen, T. B. (2018). Seeking excellence: An evaluation of 235 international laboratories conducting water isotope analyses by isotope-ratio and laser-absorption spectrometry. Rapid *Commun Mass Spectrom. 32,* 393- 406. https://doi.org/10.1002/rcm.8052

60. Wen, M., He, D., Li, M., Ren, R., Jin, J. and Si, B. (2022). Causes and factors of cryogenic extraction biases on isotopes of xylem water. *Water Resources Research, 58*(8), p.e2022WR032182. https://doi.org/10.1029/2022WR032182

61. Yang, B., Dossa, G. G., Hu, Y., Liu, L., Meng, X., Du, Y., Li, J. P., Zhu, X., Zhang, Y., Singh, A. K., Yuan, X., Jian, W., Zakari, S., Liu, W., and Song, L. (2023). Uncorrected soil water isotopes through cryogenic vacuum distillation may lead to a false estimation on plant water sources. *Methods in Ecology and Evolution*, *14*(6), 1443–1456. https://doi.org/10.1111/2041-210x.14107

62. Younger, S. E., Blake, J., Jackson, C. R., and Aubrey, D. P. (2024). δ2H isotopic offsets in xylem water measurements under cryogenic vacuum distillation: Quantifying and correcting wood-water hydrogen exchange influences. *Ecohydrology, 17*(3*),* e2640. https://doi.org/10.1002/eco.2640

63. Zuecco, G., Amin, A., Frentress, J., Engel, M., Marchina, C., Anfodillo, T., Borga, M., Carraro, V., Scandellari, F., Tagliavini, M. Zanotelli, D., Comiti, F. and Penna, D. (2022). A comparative study of plant water extraction methods for isotopic analyses: Scholander-type pressure chamber vs. cryogenic vacuum distillation. *Hydrology and Earth System Sciences, 26*(13), pp.3673-3689. https://doi.org/10.5194/hess-26-3673-2022